

JPET#49601

The cytochrome P450 2B6 is the main catalyst of efavirenz primary and secondary metabolism: implication for HIV/AIDs therapy and utility of efavirenz as substrate marker of CYP2B6 catalytic activity.

Bryan A Ward, J Christopher Gorski, David R Jones, Stephen D Hall, David A Flockhart, Zeruesenay

Desti.

Department of Medicine, Division of Clinical Pharmacology, Indiana University School of Medicine,

Indianapolis, IN

JPET#49601

Running title: CYP2B6 is the primary catalyst of efavirenz 8-hydroxylation.

Corresponding author:

Zeruesenay Desta, Ph.D.

Assistant Professor of Medicine and Pharmacology

Division of Clinical Pharmacology, Department of Medicine

Indiana University School of Medicine

1001 West 10th Street, WD Myers Bldg., W7123

Indianapolis, IN 46202

Telephone: (317) 630 8860 **Fax:** (317) 630 8185

E-mail: zedesta@iupui.edu

The number of:

Text pages	25
Tables	4
Figures	13
References	40
Words in the abstract	257
Words in the introduction	746
Words in the discussion	1521

Abbreviations: CYPs, cytochrome P450s; HLMS, human liver microsomes; HPLC, high performance liquid chromatography

Recommended section assignment: Absorption, distribution, metabolism and excretion

Abstract

We used human liver microsomes (HLMs) and recombinant cytochrome P450s (CYPs) to identify the routes of efavirenz metabolism and the CYPs involved. In HLMs, efavirenz undergoes primary oxidative hydroxylation to 8-hydroxyefavirenz (major) and 7-hydroxyefavirenz (minor) and secondary metabolism to 8,14-dihydroxyefavirenz. The formation of 8-hydroxyefavirenz in two HLMs showed sigmoidal kinetics (average apparent K_m , 20.2 μ M; V_{max} , 140pmol/min/mg protein; and Hill coefficient, 1.5), while that of 7-hydroxyefavirenz formation was characterized by hyperbolic kinetics (K_m , 40.1 μ M and V_{max} , 20.5pmol/min/mg protein). In a panel of 10 CYPs, CYP2B6 formed 8-hydroxyefavirenz and 8,14-dihydroxyefavirenz from efavirenz (10 μ M) at the highest rate. The K_m value for the formation of 8-hydroxyefavirenz in CYP2B6 derived from hyperbolic equation (12.4 μ M) was close to that obtained in HLMs (K_m , 20.2 μ M). None of the CYPs tested showed activity towards 7-hydroxylation of efavirenz. When 8-hydroxyefavirenz (2.5 μ M) was used as a substrate, 8,14-dihydroxyefavirenz was formed by CYP2B6 at the highest rate, and its kinetics showed substrate inhibition (K_{si} , ~94 μ M in HLMs and ~234 μ M in CYP2B6). In a panel of 11 HLMs, 8-hydroxyefavirenz and 8,14-dihydroxyefavirenz formation rates from efavirenz (10 μ M) correlated significantly with the activity of CYP2B6 and CYP3A. ThioTEPA (50 μ M) inhibited the formation rates of 8-hydroxyefavirenz and 8,14-dihydroxyefavirenz from efavirenz (10 μ M) by \geq 60% (HLMs) and $>$ 70% (CYP2B6), with K_i values $<$ 4 μ M. In conclusion, CYP2B6 is the principal catalyst of efavirenz sequential hydroxylation. Efavirenz systemic exposure is likely to be subject to interindividual variability in CYP2B6 activity and to drug interactions involving this isoform. Efavirenz may be a valuable phenotyping tool to study the role of CYP2B6 in human drug metabolism.

JPET#49601

Efavirenz [(S)-6-chloro-4-(cyclopropylethynyl)-1,4-dihydro-4-(trifluoromethyl)-2H-3,1-benzoxazin-2-one] belongs to the non-nucleoside HIV-1 reverse transcriptase inhibitor class of drugs. By binding to reverse transcriptase (RT) noncompetitively, efavirenz alters the function of this enzyme and renders it incapable of converting viral RNA to DNA. Efavirenz has gained a definitive and important place in the treatment of HIV-1/AIDs as part of combination therapy. Its long half-life (~40-55 h after repeated dosing) (Smith et al., 2001) allows a durable, long-lasting reduction in HIV RNA after once-a-day dosing (600 mg) (Staszewski et al., 1999), presenting an advantage for treatment compliance and efficacy. Efavirenz is widely distributed in body compartments and is likely to be effective in protected tissues such as the central nervous system and testes (Wynn et al., 2002), (Taylor et al., 2001). Recent clinical trials suggest that efavirenz has favorable effects on lipid profiles (McComsey et al., 2003), which make it an important drug to replace (switch from) protease inhibitor - based therapy to minimize the consequences of hyperlipidemia.

However, the use of efavirenz is associated with variable response: genotypic viral resistance and failure of therapy in some patients (Marzolini et al., 2001), (Langmann et al., 2002) and CNS adverse effects in a substantial number of patients (up to 50%) (Marzolini et al., 2001). Studies have shown that the plasma concentrations of efavirenz predict its efficacy and CNS adverse effects: patients with subtherapeutic plasma concentrations (<1mg/L) appear to be at greater risk for development of drug resistance and treatment failure (Langmann et al., 2002), (Marzolini et al., 2001) and those with plasma concentrations over 4mg/L are at increased risk of CNS side effects (Marzolini et al., 2001). Therefore, it appears important to maintain maximum virally suppressive efavirenz concentrations that will prevent the emergence of resistance, while also ensuring an adverse event profile that is not only safe, but does not significantly compromise overall quality of life. Achieving this goal has become increasingly difficult, in part because the pharmacokinetics of efavirenz varies widely among individuals (Smith et al., 2001), (Marzolini et al., 2001), and probably for this reason, the severity of drug interactions with efavirenz is variable and unpredictable (Smith et al., 2001), (Lopez-Cortes et al., 2002). The propensity for drug interactions with efavirenz is particularly very high which needs due attention. Efavirenz is

JPET#49601

always used in combination therapy, frequently in the presence of herbal and nutritional supplements or in concert with drugs directed at the treatment of opportunistic infections and other HIV-related disorders. Efavirenz, being a substrate (Smith et al., 2001), (Mutlib et al., 1999), an inhibitor (Von Moltke et al., 2001) and an inducer of P450s (Mouly et al., 2002), exhibits multiple interactions with the CYP450 system. Evaluation of drug interactions with efavirenz is further complicated as efavirenz is reported to enhance its own metabolism during repeated administration (Smith et al., 2001). In order to predict and identify factors that alter efavirenz pharmacokinetics, drug interaction and response, it is important to thoroughly understand the mechanisms underlying intersubject variability in efavirenz systemic exposure.

Efavirenz is extensively metabolized in humans by the cytochrome P450 (CYP) system to inactive hydroxylated metabolites that include 8- and 7-hydroxyefavirenz, with subsequent urinary and biliary excretion of these metabolites after conjugation (mainly glucuronidation) (Mutlib et al., 1999). It follows that variable activity of the specific CYPs involved in efavirenz metabolism may account for the substantial interindividual variability in efavirenz pharmacokinetics. The safe and effective use of this drug largely depends on our ability to unequivocally identify the CYPs involved and determine the precise contribution of each isoform in efavirenz metabolism. The product label of efavirenz (Product information, 2002) and review articles (Smith et al., 2001) implicate CYP3A and CYP2B6 in efavirenz metabolism, but there has been no published data that comprehensively address the contribution of these or any other enzymes *in vitro* or *in vivo*. According to Mouly et al. (Mouly et al., 2002), there was no correlation between efavirenz systemic exposure and hepatic CYP3A activity in humans. It is also important to note that clarithromycin, a known inhibitor of CYP3A in the gut-wall and the liver (Gorski et al., 1998), had little effect on the elimination of efavirenz in healthy volunteers (Product information, 2002). Recently, Chen et al have shown that CYP2B6 is the principal catalyst of the *in vitro* metabolism of DPC 963 (Chen et al., 2003), another non-nucleoside reverse transcriptase inhibitor that is structurally similar to efavirenz. All these data suggest that CYPs (most likely CYP2B6) other than CYP3A might be responsible for the human metabolism of efavirenz.

JPET#49601

The primary objective of the present study was to identify the mechanisms underlying interindividual variability in efavirenz pharmacokinetic and drug interactions. Using human liver microsomes (HLMs) and recombinant CYPs, we determined the primary and secondary metabolism of efavirenz and the specific CYPs involved. We also tested the utility of efavirenz as a novel substrate probe of CYP2B6. This enzyme system does play an important role in the metabolism of a growing list of frequently prescribed drugs and other chemicals (Wang and Halpert, 2002),(Ekins and Wrighton, 1999), but it has been studied less because of unavailability of a specific and safe substrate reaction marker that will allow prediction of *in vivo* activity from *in vitro* studies.

Material and Methods

Chemicals: Efavirenz was obtained from Dupont Pharmaceuticals Company (Wilmington, DE).

Ritonavir was obtained from Abbot Laboratories (North Chicago, IL). 8-Hydroxyefavirenz was a generous gift of Dr. David Christ of the MAP Wilmington (Dupont Pharmaceuticals Company, Experimental Station, Wilmington, Delaware). Quinidine, diethyldithiocarbamate, troleandomycin, ketoconazole, glucose 6-phosphate, glucose-6-phosphate dehydrogenase, and β -NADP were purchased from Sigma Chemical Co. (St. Louis, MO). Sulfaphenazole and furafylline were obtained from Ultrafine Chemicals (Manchester, England). ThioTEPA was purchased from the U. S. Pharmacopoeia Convention (Rockville, MD). Omeprazole was a generous gift from Dr. Tommy Anderson (Clinical Pharmacology, Astra Hässle AB, Mölndal, Sweden). All other chemicals and solvents were of HPLC grade.

Microsomal preparations: The human liver microsomes (HLMs) that we used were prepared from human liver tissues that were medically unsuitable for transplantation. Microsomal fractions were prepared by ultracentrifugation using standard protocols as described elsewhere (Desta et al., 1998), and protein concentrations were determined by the Bradford method (Bradford, 1976) using BSA as a standard. The microsomal pellets were suspended in a reaction buffer to a protein concentration of 10 mg/ml (stock) and were kept at -80°C until used. Additional HLMs, baculovirus-insect cell expressed human P450s (1A2, 2A6, 2B6, 2C8, 2C9, 2C19, 2D6, 2E1, 3A4 and 3A5) (with oxido-reductase) and cytochrome b5 were purchased from GENTEST (Woburn, MA). The microsomal preparations were stored at -80°C until use. The total P450 content, protein concentrations and the specific activity of each P450 isoform were as supplied by the manufacturer.

Incubation conditions and HPLC assay: Pilot incubation experiments were performed in HLMs to identify potential oxidative metabolites, and to optimize conditions for incubation and HPLC analysis. Efavirenz was dissolved in methanol and serially diluted in methanol to the required concentration. Any methanol was removed by drying in speed vacuum before reconstituting the residue with phosphate buffer and addition of other incubation components. For the pilot studies, efavirenz ($10\mu\text{M}$) and a NADPH-generating system (13 mM NADP,

JPET#49601

33 mM glucose 6-phosphate, 33 mM MgCl₂, and 0.4 U/ml glucose 6-phosphate

dehydrogenase) in potassium phosphate buffer (pH, 7.4) were allowed to equilibrate for 5 min at 37°C. After the reaction was initiated by adding 25 µl of HLMs (10 mg protein/ml) and incubated for 30 min at 37°C (final volume, 250 µl), the reaction was terminated by placing tubes on ice and immediately adding 500 µl of acetonitrile. Ritonavir (50µl of 0.01mg/ml) was added as an internal standard to the incubation sample, vortex-mixed and centrifuged at 14,000 rpm for 5 min in an Eppendorf model 5415C centrifuge (Brinkman Instruments, Westbury, NY). The supernatant was removed to a clean tube and extracted twice using ethyl acetate under alkaline pH (0.5mL of 0.5M NaOH, adjusted to pH=10 using 1% phosphoric acid). The organic phase was removed and evaporated to dryness. The residue was reconstituted with 150 µl mobile phase, and 100µl was injected onto HPLC system (see below). Negative control incubations were run in parallel that included exclusion of efavirenz, a NADPH-generating system or microsomes (BSA was used instead) from the incubation mixture.

An HPLC assay method with UV detection was developed for the quantification of efavirenz and its metabolites. The HPLC system consisted of a Waters Assoc. model 515 pump (Milford, MA), model 717 autosampler, and model 490 programmable absorbance UV detector. The separation system consisted of a Zorbax SB-C₁₈ column (150x4.6mm, 3.5-micron particle size, Phenomenex® Torrance, CA), a Luna C₁₈ Guard column (30x4.6 mm, 5 µ, Phenomenex® Torrance, CA), and a mobile phase composed of 55% 10 mM KH₂PO₄ (adjusted to pH 2.4 with 1% phosphoric acid) and 45% v/v acetonitrile (flow rate, 0.8 ml/min). The column eluate was monitored by UV detection at 245 nm. Efavirenz and its metabolites were quantified by using the ratio of peak area of the metabolite to peak area of internal standard and calibration curves that were constructed using known efavirenz concentrations. Although we recognize that standard curves constructed using synthetic metabolite references provide optimal quantification of efavirenz metabolism, we used efavirenz standard curves for quantification because we had initially no access to the metabolites of efavirenz or the amount were not enough to construct repeated standard curves. Of note, when equimolar concentration (10µM) of 8-hydroxyefavirenz and efavirenz were directly injected to the HPLC system, the difference in UV activity

JPET#49601

between 8-hydroxyefavirenz and efavirenz was minimal (5%). At 1 and 10 μ M efavirenz, the interday and intraday coefficient of variance of the assay was less than 10% and 4% respectively.

Using the incubation and HPLC assay conditions described above, three well-separated chromatographic HPLC peaks were noted in the incubation mixture consisting of efavirenz, a NADPH-generating system and HLMs (but not in the negative control experiments). Linearity in the formation rate of these metabolites was established with regard to microsomal protein concentrations and incubation time. Efavirenz (10 μ M) was incubated in HLMs (0-1.5 mg protein /ml) and a NADPH generating system at 37°C across a range of incubation times (0-75 min). Based on the results obtained, linear conditions for efavirenz incubation consisted of 30 min incubation and a final protein concentration of 0.5 mg/ml, and were used in subsequent experiments responsible for efavirenz metabolism unless otherwise stated.

Identification of efavirenz metabolites: We used two approaches to obtain structural evidence for the metabolites of efavirenz in microsomal incubates. First, retention times of efavirenz metabolite peaks after injection of microsomal incubates of efavirenz in to HPLC system were compared with that of reference metabolite standard (8-hydroxyefavirenz). The retention time of 8-hydroxyefavirenz was determined after direct injection or after adding it to incubation mixture that did not contain active microsomes. Second, we used liquid chromatography-mass spectrometry (LC/MS) analysis. Efavirenz (10 μ M) was incubated with NADPH and HLMs for 30 min at 37°C, and the reaction was terminated and processed as described above. Peaks of interest were separated on a Luna 3 μ C18-2 column (100 x 2.00 mm id; Phenomenex; Torrence, CA). The eluate was delivered at a rate of 0.2 ml/min with out splitting to an ESI probe. LC/MS analysis was performed in the extracted samples to determine the MS fragmental pattern. The LC/MS was performed using a ThermoFinnigan AQA mass spectrometer (San Jose, CA) equipped with a ThermoFinnigan HPLC system which consisted of an autosampler (AS3000), binary pump (P4000) and a photodiode array detector (UV6000LP). Mass spectrometer settings were as follows: cone voltage (29 Volts); probe voltage 4.00 V; and probe temperature 350°C. A

JPET#49601

gradient elution profile was used to separate the metabolites. Initial mobile phase was 75% ammonium formate (adjusted to pH 3.5 with formic acid) with 25% acetonitrile. One minute after the start of the run, the acetonitrile percentage was increased linearly over 19 minutes to 80% and held for 8 minutes. Then, initial mobile phase conditions were resumed after 4 minutes. The column was allowed to equilibrate for 5 minutes between injections. Data were collected in negative ESI mode (SIM and SCAN). The MS fragmentation patterns obtained were compared with those from urinary metabolite profiles of efavirenz described in humans (Mutlib et al., 1999) and with those of synthetic standards of efavirenz and its metabolite.

Kinetic analyses in HLMs. Kinetic studies for efavirenz metabolism were conducted in two different human liver microsomal preparations. Efavirenz (0.1-200 μM) was incubated in duplicate for 30 min at 37°C with HLMs (0.5 mg protein/ml) and a NADPH-generating system, and the reaction was terminated and processed as described above. The formation rates of metabolites vs. efavirenz substrate concentrations were fit to hyperbolic and non-hyperbolic enzyme kinetic models in order to estimate apparent kinetic parameters (e.g. K_m and V_{max} ; see Data Analysis Section).

Correlation experiments. Efavirenz (10 μM) was incubated with microsomes from 11 different livers to test the correlation of efavirenz metabolism with the activity of individual CYP. The total P450 contents, oxidoreductase, and the activity of each P450 isoform were as supplied by the manufacturer (Gentest, Woburn, MA). Isoform-specific reaction markers were used to determine the activity of each CYP: phenacetin O-deethylase (CYP1A2), coumarin 7-hydroxylase (CYP2A6), S-mephenytoin N-demethylation (CYP2B6), paclitaxol 6 α -hydroxylase (CYP2C8), diclofenac 4'-hydroxylation (CYP2C9), S-mephenytoin 4'-hydroxylation (CYP2C19), bufuralol 1'-hydroxylation (CYP2D6), chlorzoxazone 6-hydroxylation (CYP2E1), testosterone 6 β -hydroxylation (CYP3A) and lauric acid 12-hydroxylation (CYP4A) (see www.gentest.com). The correlation coefficients between the formation rates of efavirenz metabolites and the activity of each CYP isoform in different HLMs were calculated by nonparametric regression analysis (Spearman's rank correlation test) with GraphPad Prism Software (Version 3.1, San Diego, CA). $P < 0.05$ is considered statistically significant.

JPET#49601

Inhibition studies: The rates of efavirenz (10 μ M) metabolism in HLMS were evaluated in the absence (control) and presence of the following known isoform-specific inhibitors: furafylline (20 μ M) for CYP1A2, sulfaphenazole (20 μ M) for CYP2C9, omeprazole (10 μ M) for 2C19, quinidine (1 μ M) for CYP2D6, troleandomycin (50 μ M) and ketoconazole (1 μ M) for CYP3A, diethyldithiocarbamate (50 μ M) for CYP2E1 and thioTEPA (50 μ M) for CYP2B6. The specific conditions used with these inhibitors have been described in detail in earlier publications (Desta et al., 1998), (Rae et al., 2002). Efavirenz was incubated in HLMS (0.5 mg/ml) with or without CYP isoform-specific inhibitor and with an NADPH regenerating system for 30 min. Troleandomycin, furafylline, and diethyldithiocarbamate were preincubated with a NADPH regenerating system and HLMS for 15 min at 37°C before initiation of the reaction by addition of efavirenz and further incubation for 30 min. The inhibition (%) of metabolite formation rate by P450 isoform-specific inhibitors was calculated by comparing the inhibited activity with uninhibited controls (without inhibitors).

The inhibition data identified thioTEPA as the only potent inhibitor of efavirenz metabolism (with no marked effects by other inhibitors). Subsequent experiments were designed to further characterize this inhibition. A single concentration of efavirenz (10 μ M) was incubated without or with multiple thioTEPA concentrations (1-25 μ M) in HLMS and a NADPH-generating system. The data obtained from this experiment were used to calculate IC₅₀ and to simulate appropriate ranges of efavirenz and thioTEPA concentrations to construct Dixon plots to estimate K_i values for the inhibition of efavirenz metabolism. Efavirenz concentration ranged from 5 to 25 μ M and thioTEPA ranged from 0 to 10 μ M. The inhibition data were modeled using appropriate enzyme inhibition equations (see Data Analysis).

An earlier report (Rae et al., 2002) suggests that thioTEPA inhibits S-mephenytoin N-demethylation, an *in vitro* substrate probe of CYP2B6 (Ko et al., 1998), in time-dependent manner. Thus, the time-dependent inhibition of efavirenz metabolism by thioTEPA was also tested. ThioTEPA (5 μ M) was incubated with HLMS and a NADPH-generating system for 0 to 30 min before the reaction was initiated by addition of efavirenz (10 μ M) and further incubated for 30 min. To determine if thioTEPA caused metabolite intermediate complex

JPET#49601

(MIC) formation, thioTEPA (50 μ M) was incubated in pooled HLMs (1 mg/ml) and recombinant human CYP2B6 (200 pmols/ml). MIC formation was characterized by dual wavelength spectroscopy [Uvikon 933 double beam UV/VIS Spectrophotometer; Research Instruments International, San Diego CA] by scanning from 380 nm-500 nm as described in detail elsewhere (Jones et al., 1999).

Metabolism of efavirenz by recombinant human CYP450 isoforms: To further identify the specific P450 isoforms catalyzing the metabolism of efavirenz, recombinant human CYP 1A2, 2A6, 2B6, 2C8, 2C9, 2C19, 2D6, 2E1, 3A4 or 3A5 (13 pmol each) were incubated with efavirenz (1, 10 and 100 μ M) and a NADPH-generating system (same composition as above) at 37°C for 30 min. All other incubation conditions and assay of the metabolites were the same as described for HLMs above. The rates of formation of efavirenz metabolites as well as the amount of efavirenz remaining in the microsomal incubates after 30 min incubation relative to the initial concentrations added were calculated.

For those CYPs showing activity towards efavirenz metabolism, full kinetic analyses were performed. Efavirenz (0-200 μ M) was incubated with 13 μ l of 1 nmol of P450/ml (recombinant human CYP2B6, CYP1A2, CYP3A4 and CYP3A5). To test whether the presence of cytochrome b5 modifies the kinetics of efavirenz metabolism by CYP2B6, 0-150 μ M efavirenz was incubated with CYP2B6 (13 μ l of 1 nmol CYP2B6/ml) that was expressed with cytochrome b5. The kinetic parameters were obtained using hyperbolic and non-hyperbolic enzyme kinetic equations (see Data Analysis).

Sequential metabolism of efavirenz: Our LC/MS data indicated that one of the three efavirenz metabolite peaks is consistent with a dihydroxylated metabolite of efavirenz, suggesting that it might represent a secondary metabolite. Thus, we conducted experiments to systematically test this possibility. First, we determined the time course for the formation of each metabolite from efavirenz in HLMs. Efavirenz (5 μ M) was incubated in HLMs (0.5mg/ml) and a NADPH generating system (final volume, 250 μ M) at 37°C. Reaction was terminated at time = 0 and after 5, 10, 15, 20, 30, 45, 60, 90 and 120 min of incubation. Second, we tested whether MIII might be formed when 8-hydroxyefavirenz is incubated in HLMs. Efavirenz is believed to undergo relatively rapid 8-

JPET#49601

hydroxylation in humans (Mutlib et al., 1999), raising the possibility that the secondary metabolite is formed from efavirenz through step-wise hydroxylation with 8-hydroxyefavirenz as an intermediate. Thus, 8-hydroxyefavirenz (10 μ M) was incubated with HLMs (0.5 mg/ml) and a NADPH-generating system at 37°C for 30 min, and reaction was terminated by addition of 500 μ l acetonitrile. Appropriate negative controls and efavirenz (10 μ M) incubation experiments were also performed in parallel. Extraction protocols and HPLC assay were similar to those described above for efavirenz. The retention time of the metabolite peak formed from 8-hydroxyefavirenz microsomal incubation was compared with those produced when efavirenz was used as a substrate. LC-MS analysis was performed according to the protocol described for efavirenz metabolites (see above). These data suggested that dihydroxyefavirenz is formed when both efavirenz and 8-hydroxyefavirenz were used as substrates. Third, since our studies with recombinant human CYPs indicated that the formation of the dihydroxyefavirenz from efavirenz is dependent on CYP2B6, we tested if the same enzyme also catalyzes the conversion of 8-hydroxyefavirenz to dihydroxyefavirenz. 8-Hydroxyefavirenz (2.5 μ M) was incubated in HLMs or a panel of cDNA expressed human CYPs (13 pmol each) and a NADPH generating system for 30 min at 37°C. The formation rates of dihydroxyefavirenz and the disappearance of 8-hydroxyefavirenz from microsomal incubate was quantified. Fourth, we determined full kinetic analysis for the formation of dihydroxyefavirenz from 8-hydroxyefavirenz in HLMs and CYP2B6. 8-Hydroxyefavirenz (0-200 μ M) was incubated in HLMs (0.5 mg/ml) (or CYP2B6, 52 pmol P450/ml) and a NADPH-generating system. The formation rates of dihydroxyefavirenz vs. 8-hydroxyefavirenz concentrations were fit to appropriate enzyme kinetic models to estimate kinetic parameters (see Data Analysis Section).

Data Analysis: Estimates of kinetic constants were obtained by nonlinear regression analysis using WinNonlin (Software Version 4.0; Pharsight, Mountain View, CA). The simple single-site Michaelis-Menten equation ($V = V_{\max} * C / (K_m + C)$), Hill equation ($V = V_{\max} * C^n / (C_{50} + C^n)$), or substrate inhibition equation ($V = V_{\max} / (1 + K_m / C + C / K_{si})$) were fitted to formation rates (V) of efavirenz metabolites versus efavirenz (or 8-hydroxyefavirenz) concentrations (C). The apparent maximum formation rate (V_{\max}), and apparent substrate

JPET#49601

concentration resulting in 50% of V_{\max} , Hill coefficient (n) and substrate inhibition constant

(K_{si}) were calculated. *In vitro* intrinsic clearances (Cl_{int}) were given as V_{\max}/K_m or V_{\max}/K_m^n . Inhibition constants (K_i values) were estimated from the inhibition data using nonlinear regression for the noncompetitive inhibition model using WinNonlin. The models that best fit were selected based on the dispersion of residuals and standard errors of the parameter estimates. Kinetic constants were given as mean \pm SD (or \pm SE of parameter estimates).

Results

Efavirenz metabolism in HLMs and identification of metabolites. A typical HPLC chromatogram of efavirenz and its metabolites in human liver microsomal incubate is shown in Figure 1. Two major metabolite peaks designated as MI and MIII were separated at retention times of 15.80 ± 0.04 min and 8.30 ± 0.03 min respectively. A minor metabolite peak was identified at 13.20 ± 0.02 min. Ritonavir (internal standard) and efavirenz appeared at retention times of 17.2 ± 0.13 and 27.20 ± 0.08 min respectively. The formations of all three metabolites were dependent on NADPH regenerating system, duration of incubation, and microsomal protein and efavirenz concentrations. The peak eluting at 4.2 min (Fig. 1) was related neither to efavirenz nor to the internal standard as it was still observed in microsomal incubations with no efavirenz or when ritonavir was not added to the microsomal incubates.

The identity of the metabolite peaks shown in Figure 1 was confirmed by comparison of LC retention times with synthetic reference compounds and LC/MS analysis. When we compare the HPLC retention times of efavirenz metabolite peaks in microsomal incubates with that of 8-hydroxyefavirenz, the retention time of MI (15.80 ± 0.04 min) coeluted with that of 8-hydroxyefavirenz (15.80 ± 0.01 min). The LC/MS fragmentation patterns were compared with previously published fragmentation patterns of efavirenz metabolism *in vivo* (Mutlib et al., 1999). The major metabolite peak (MI) obtained following incubation of efavirenz with HLMs (LC retention time, 18 min) had characteristic ions at 330 m/z; 286 m/z and 258.0 m/z, consistent with the fragmentation pattern of 8-hydroxyefavirenz. A smaller peak (MII) from efavirenz incubation with a retention time of 17.2 min showed characteristic ions at 258.0 m/z and 330 m/z that concur with 7-hydroxyefavirenz. MIII had characteristic ions at 346 m/z, 302 m/z and 274 m/z, consistent with 8,14-dihydroxyefavirenz. In this *in vitro* study, 8-hydroxylation to 8-hydroxyefavirenz (MI), 7-hydroxylation to 7-hydroxyefavirenz (MII) and 8,14-dihydroxyefavirenz (MIII) were identified as efavirenz oxidative metabolites.

JPET#49601

In figure 2, the time course for the formation of efavirenz metabolites is depicted.

The formation of 8,14-dihydroxyefavirenz showed a significant lag-time relative to the formation of 8-hydroxyefavirenz. These data together with the results from LC/MS analysis suggest that 8,14-dihydroxyefavirenz is a secondary metabolite of efavirenz. It is unlikely that 8- and 14-hydroxylation occurs simultaneously. There are two possible routes for the formation of 8,14-dihydroxyefavirenz from efavirenz: 1) efavirenz undergoes 14-hydroxylation first followed by 8-hydroxylation of the product or (2) 8,14-dihydroxyefavirenz is formed via a step-wise hydroxylation of efavirenz, with 8-hydroxyefavirenz as an intermediate. Although it was not determined experimentally, there are reasons to believe that the first possibility is unlikely. In vivo studies indicate that 8-hydroxyefavirenz is the main metabolite and is rapidly formed from efavirenz in humans, but there is no evidence that 14-hydroxyefavirenz is formed (Mutlib et al., 1999). To test the second possibility, we incubated 8-hydroxyefavirenz (2.5 μ M) in HLMs (HL9) and monitored the formation of 8,14-dihydroxyefavirenz. Indeed, 8-hydroxyefavirenz was efficiently metabolized to 8,14-dihydroxyefavirenz ($V = 52.7$ pmol/min/mg protein). Collectively, our data provide evidence that 8,14-dihydroxyefavirenz is formed from efavirenz by step-wise hydroxylation, i.e., first 8-hydroxyefavirenz is formed followed by further 14-hydroxylation: significant quantity of both the primary and the secondary metabolites were detected when efavirenz is used as a substrate (Fig. 1); the formation of 8,14-dihydroxyefavirenz (but not that of 8-hydroxyefavirenz) behaved as a secondary metabolite because the time course for its formation was characterized by a significant lag-time; and more importantly 8,14-dihydroxyefavirenz was formed efficiently when 8-hydroxyefavirenz was used as a substrate. Assuming the metabolites have similar UV-absorbance intensity at equi-molar concentrations, the data in Figure 1 and the time course profile (Fig. 2) suggest that the 8-hydroxylation pathway (formation of 8-hydroxyefavirenz + its sequential metabolism to 8,14-dihydroxyefavirenz) represents a major route of efavirenz metabolism (over 92% of efavirenz oxidation), while the contribution of 7-hydroxylation appears to be small (<8%).

JPET#49601

Kinetic analysis in HLMs: Kinetic analysis of efavirenz metabolite formation rates

was performed in two different HLM preparations. The kinetic parameters estimated are summarized in Table 1. The kinetic profiles of efavirenz metabolism to 8-hydroxyefavirenz in HLMs (HL9 and HL9/14/99) are shown in Figure 3. The formation rate of 8-hydroxyefavirenz revealed sigmoidal saturation curves (Fig. 3, left panel) that were fit to a Hill equation ($n=1.33$ in HL9 and 1.72 in HL9/14/99) (Table 1). The Eadie-Hofstee plots [V] and V/S (substrate concentration)] of this metabolite showed curvilinear relationships (Fig. 3, right panel), indicating positive cooperativity. The formation rate of 7-hydroxyefavirenz in HLMs was characterized by a hyperbolic saturation curve and an Eadie-Hofstee plot that was linear (data not shown), suggesting the involvement of a single enzyme or more than one enzyme with similar affinity. The *in vitro* intrinsic clearance (Cl_{int}) for the formation of 8-hydroxyefavirenz was 17- and 14-fold higher in HL9 and HL9/14/99 respectively than that for 7-hydroxyefavirenz. Of note, the Cl_{int} for the formation of 8-hydroxyefavirenz described here is clearly underestimated because it does not account for the sequential metabolism. The fold difference in Cl_{int} between the formation rate of 7-hydroxyefavirenz and the total 8-hydroxylation pathway (8-hydroxyefavirenz + 8,14-dihydroxyefavirenz) is therefore expected to be large than that provided here.

The formation rate of 8,14-dihydroxyefavirenz vs. 8-hydroxyefavirenz concentrations was characterized by an initial rapid increase at lower substrate concentrations followed by a progressive decline at higher substrate concentrations (Fig. 4). Comparison of the goodness-of-fit values generated from these data indicates that a substrate inhibition equation enzyme model provided a better fit than other models. The corresponding Eadie-Hofstee plot indicated a “hook” in the upper region of this plot (Fig. 4, insert), which is characteristic of substrate inhibition. The K_m (μM), V_{max} (pmol/min/mg protein) and K_{si} (μM) estimated from these data respectively were 0.78, 27.66 pmol/min/mg protein and 94 μM . When efavirenz was used as a substrate, the formation of 8,14-dihydroxyefavirenz in HLMs showed essentially similar kinetic profiles as that described when 8-hydroxyefavirenz was used as a substrate (K_m (μM), V_{max} (pmol/min/mg protein) and K_{si} (μM) estimated respectively were 6.6, 66 pmol/min/mg protein and 278 μM in HL HL9/14/99 and 2.2, 30 and 91 in HL9).

JPET#49601

Although these data provided valuable information on what might be expected with respect to the formation of 8,14-dihydroxyefavirenz from efavirenz, the fact that 8,14-dihydroxyefavirenz is formed from efavirenz by a two-step reaction would mean that the kinetic parameters generated for the formation of this metabolite using efavirenz as a substrate is likely to be compromised by the rate of the first hydroxylation (8-hydroxylation) and the second hydroxylation (14-hydroxylation).

Correlation analysis: Figure 5 shows the rate of efavirenz (10 μ M) metabolism in a panel of 11 characterized HLMs. We assessed the formation rates of 8-hydroxyefavirenz and 8,14-dihydroxyefavirenz independently and as a summation. The average formation rates (pmol/min/mg protein) of efavirenz (10 μ M) metabolism to 8-hydroxyefavirenz, 7-hydroxyefavirenz, 8,14-dihydroxyefavirenz, and 8-hydroxyefavirenz +8,14-dihydroxyefavirenz in a panel of 11 HLMs were 38.7 \pm 24.5 (range: 10.8 to 83.1; 7.7-fold), 2.8 \pm 1.9 (range: 0 to 4.4), 9.5 \pm 9.7 (range: 2.4 to 13.9; 13.4-fold), and 48.3 \pm 33.9 (range: 13.6 to 114.1; 8.4-fold) respectively. 7-Hydroxyefavirenz was not detected in one of the HLMs, but in the 10 HLMs where this metabolite was detected, variability between HLM preparations was low (3.5-fold). The summation of 8-hydroxyefavirenz and 8,14-dihydroxyefavirenz formation rates were significantly correlated with the formation rate of 8-hydroxyefavirenz ($r=0.999$, $p=0.0001$) and 8,14-dihydroxyefavirenz ($r=0.83$, $p<0.0047$). 7-Hydroxyefavirenz formation rates did not correlate with the other metabolites ($r<0.2$; $p>0.7$). In the panel of HLMs tested, 17.1 \pm 5.3% (range: 8.8 to 28.8; 3.3-fold) of the total rate was accounted for 8,14-dihydroxyefavirenz formation from 8-hydroxyefavirenz, while 82.9 \pm 5.3% (range: 71.2 to 91.1; 1.3-fold) was accounted for the remaining 8-hydroxyefavirenz formation rate. Assuming that 8,14-dihydroxyefavirenz is not further metabolized, it seems that the formation rates of 8-hydroxyefavirenz might be underestimated by <20%.

Correlations between the rate of efavirenz metabolism and the activities CYPs and total P450 contents in HLMs are summarized in Table 2. The formation rates of 8-hydroxyefavirenz and 8,14-dihydroxyefavirenz correlated significantly with the activity of CYP3A, CYP2B6 and total P450 content. In addition, CYP2C8 showed weak but significant correlation with the formation rate of 8-hydroxyefavirenz. When the combined

JPET#49601

formation rates 8-hydroxyefavirenz and 8,14-dihydroxyefavirenz were analyzed, the correlation was similar to the correlations noted with 8-hydroxyefavirenz alone (Table 2). The formation rate of 7-hydroxyefavirenz was correlated with none of the P450s tested, except a tendency for CYP4A ($r=0.6$; $p=0.07$).

Metabolism of efavirenz by recombinant human CYPs: Three concentrations of efavirenz (1 μ M, 10 μ M and 100 μ M) were incubated with a panel of recombinant P450s. At 1 μ M efavirenz, CYP2B6 significantly reduced the concentration of efavirenz in the microsomal incubates (by about 96%) relative to other isoforms or incubations that do not contain microsomes (instead bovine serum albumin was used) (data not shown). The formation rates (pmol product/min/pmol of P450) of 8-hydroxyefavirenz and 8,14-dihydroxyefavirenz after incubation of efavirenz (10 μ M) with CYPs are shown in Figure 6 (left panel). Except CYP2B6, none of the CYPs tested catalyzed the formation of 8,14-dihydroxyefavirenz. CYP2B6 formed 8-hydroxyefavirenz at the highest rate. CYP3A5, CYP1A2 and CYP3A4 also catalyzed the formation of 8-hydroxyefavirenz, but when compared with CYP2B6, the involvement of these isoforms in the formation of 8-hydroxyefavirenz was low (10.2-, 8.4- and 24-fold lower respectively). At 100 μ M efavirenz (Fig. 6; right panel), the following isoforms contributed to the formation rates (pmol/min/pmol P450) of 8-hydroxyefavirenz: CYP2B6, CYP3A5, CYP1A2, CYP 3A4, CYP2A6 and CYP2C9. These data show that CYP2B6 is 11.8-, 5.2- and 30-fold catalytically active than CYP1A2, CYP3A5 and CYP3A4 respectively towards the formation of 8-hydroxyefavirenz. CYP2B6 was also the main catalyst of 8,14-dihydroxyefavirenz formation, with small contribution of CYP2C9. Although CYP2B6 remained the main isoform responsible for efavirenz metabolism at all substrate concentrations tested, the pattern of metabolite formation varied with increasing substrate concentration. For example, 8,14-dihydroxyefavirenz was formed more efficiently at lower substrate concentrations, while 8-hydroxyefavirenz was predominant with increasing concentration of efavirenz [the formation rates of 8,14-dihydroxyefavirenz by CYP2B6 was decreased (by ~53%) from 0.496 ± 0.039 pmol/min/ pmol P450 at 10 μ M to 0.262 ± 0.014 pmol/min/ pmol P450 at 100 μ M]. These data were essentially similar to the data observed in HLMs. At any of the concentrations of efavirenz used, none of the recombinant CYPs tested formed 7-hydroxyefavirenz.

JPET#49601

Full kinetic analysis was performed for the formation rate of 8-hydroxyefavirenz from efavirenz by recombinant human CYP2B6 (Fig. 7). The formation rates of 8-hydroxyefavirenz vs. efavirenz concentration fit better to a single-site Michaelis-Menten equation. The respective data obtained are listed Table 3. In HLMs, the formation of 8-hydroxyefavirenz was characterized by sigmoidal curve (Fig. 3). Fitting the data obtained from recombinant CYP2B6 to Hill equation did not improve the estimation (Hill coefficient, 1.19 ± 0.19 ; $n=3$ experiments in duplicate determinations). The K_m values obtained in recombinant CYP2B6 ($12.4 \pm 1.8 \mu\text{M}$) (Table 3) were close to that obtained from HLMs (average from the two HLMs, $20.16 \mu\text{M}$) (Table 1), suggesting that this same enzyme is catalyzing efavirenz metabolism in both preparations. Besides CYP2B6, CYP1A2, CYP3A5 and CYP3A4 showed some activity towards the formation of 8-hydroxyefavirenz (Fig. 6). Thus, we examined the kinetics for the formation rate of 8-hydroxyefavirenz in CYP1A2, CYP3A5 and CYP3A4 and compared the data with the formation rate in CYP2B6 (Fig. 8). The respective kinetic parameters derived from fitting the data to a single-site Michaelis-Menten equation are shown in Table 3. The K_m values for the formation of 8-hydroxyefavirenz by CYP1A2, CYP3A5 and CYP3A4 were comparable with that obtained with CYP2B6, but the V_{max} values obtained from CYP1A2, CYP3A5 and CYP3A4 were much smaller compared to those obtained in CYP2B6. Accordingly, the *in vitro* intrinsic clearance ($\mu\text{l}/\text{min}/\text{picomole of P450}$) for the formation of 8-hydroxyefavirenz in CP2B6 was 5.8-, 13.5- and 60-fold higher than that of CYP1A2, CYP3A5 and CYP3A4 respectively. CYP2B6 is the main enzyme that catalyzes the formation of 8-hydroxyefavirenz from efavirenz, but this metabolite is subject to additional metabolism by the same enzyme. The Cl_{int} of for the formation of 8-hydroxyefavirenz by CYP2B6 (and the fold-difference) would be larger than listed in Table 3 when corrected for sequential metabolism.

The data in figure 6 suggested to us that CYP2B6 is the dominant enzyme responsible for the formation of 8,14-dihydroxyefavirenz from efavirenz (Fig. 6) and we have evidence that this metabolite is also formed in HLM when 8-hydroxyefavirenz is used as a substrate. We tested whether CYP2B6 catalyzes this reaction when 8-hydroxyefavirenz was used as a substrate. As shown in Figure 9A, CYP2B6 catalyzed the formation of 8,14-

JPET#49601

dihydroxyefavirenz from 8-hydroxyefavirenz at the highest rate. Other enzymes also showed some activity, but at very low rate (>29-fold lower). Accordingly, CYP2B6 (but not other enzymes) decreased the amount of 8-hydroxyefavirenz remaining in microsomal incubate by 88%. Our data from HLMs indicate that the formation of 8,14-dihydroxyefavirenz exhibit substrate inhibition (Fig. 4). Consistent with these data, the kinetics for the formation of 8,14-dihydroxyefavirenz from 8-hydroxyefavirenz was characterized by substrate inhibition equation. When the substrate-velocity curve of 8,14-dihydroxyefavirenz was modeled using the substrate inhibition model, the following kinetic parameters were estimated: K_m , 2.12 μ M; V_{max} , 8.5pmol/min/pmol P450; and K_{si} , 233.6 μ M.

Studies with CYP3A have provided useful insight into the mechanism by which substrate inhibition might occur. Cytochrome b5 may modulate the efficiency of CYP3A-mediated substrate inhibitions through enhancement of the efficiency of CYP3A4-reactive oxygen production and thus the availability of heme bound oxygen for the reaction and increasing the partition of the iron-oxygen complex towards substrate oxidation ((Schrage and Wienkers, 2001) and references therein]. Since the kinetic profiles for the formation of 8,14-dihydroxyefavirenz from efavirenz or 8-hydroxyefavirenz was similar, we determined the kinetics of 8-hydroxyefavirenz and 8,14-dihydroxyefavirenz formation from efavirenz in CYP2B6, which was enriched with cytochrome b5. We wished to test if cytochrome b5 might reverse the substrate inhibition observed for 8,14-dihydroxyefavirenz or explain differences in the kinetics observed in HLMs and CYP2B6 with respect to the formation of 8-hydroxyefavirenz. As shown in Table 3, cytochrome b5 decreased the K_m and V_{max} values for the formation of 8-hydroxyefavirenz, but Cl_{int} remained similar to that without cytochrome b5. The formation of 8,14-dihydroxyefavirenz was not influenced in a significant way by cytochrome b5.

Chemical inhibition of efavirenz metabolism: To further probe the CYP450 isoforms participating in efavirenz metabolism, 10 μ M efavirenz was incubated with CYP450 isoform-specific inhibitors in HLMs. As shown in table 2, thioTEPA (50 μ M) inhibited the rates of 8-hydroxyefavirenz and 8,14-hydroxyefavirenz formation by 65% and 75% respectively. The effect of the other inhibitors tested on the formation of 8-

JPET#49601

hydroxyefavirenz and 8,14-hydroxyefavirenz was <20%. The formation rates of 7-hydroxyefavirenz was modestly inhibited by sulfaphenazole, omeprazole and TAO, weakly inhibited by ketoconazole and quinidine, and activated by thioTEPA (Table 4). The inhibition profiles in HLMs were compared with those inhibition data in recombinant human CYP2B6 (Table 4). Consistent with the HLMs, thioTEPA (50 μ M) was the only inhibitor of the formation rates of 8-hydroxyefavirenz (by 60%) and 8,14-dihydroxyefavirenz (by 88%) in CYP2B6. Similarly, thioTEPA (0-25 μ M) inhibits the formation of 8-hydroxyefavirenz and 8,14-hydroxyefavirenz in a concentration dependent manner (IC₅₀, ~10 μ M and 5 μ M respectively). It seems that 8,14-hydroxyefavirenz is more susceptible to inhibition (by 12.4% to 18.8% at 2.5-25 μ M inhibitor) by thioTEPA than 8-hydroxyefavirenz. Compared to microsomal incubations without inhibitor, thioTEPA increased the rate of 7-hydroxyefavirenz at low concentrations (1 μ M to 10 μ M) by over 18% (peak 31%), while it showed a 49% decrease at 25 μ M (data not shown). We do not believe that the increase we noted was due to coelution of thioTEPA or its metabolites with 7-hydroxyefavirenz as no peak was observed at the retention time of 7-hydroxyefavirenz when thioTEPA was incubated alone (without efavirenz).

To estimate K_i values for the inhibition of efavirenz metabolism by thioTEPA, a range of substrate concentrations (1-25 μ M) were incubated without or with thioTEPA (2.5-10 μ M) in HLMs. Representative Dixon plots for the inhibition of 8-hydroxyefavirenz and 8,14-hydroxyefavirenz formation rate from efavirenz by thioTEPA are shown in Figure 11. The K_i values estimated by nonlinear regression using noncompetitive enzyme inhibition model were 3.0 μ M and 2.5 μ M for the formation of 8-hydroxyefavirenz and 8,14-hydroxyefavirenz respectively, and these values fall within the range of therapeutic concentrations reported for thioTEPA (1.1-18.6 μ M) during a 4-day intravenous infusion at a dose of 400 to 800 mg/m² (Kennedy et al., 1995). No Dixon plot was presented for 7-hydroxyefavirenz because thioTEPA showed activation at the substrate concentrations tested (data not shown). The inhibition of efavirenz metabolism in HLMs was time dependent, i.e. the rate of metabolism of efavirenz markedly decreased during preincubation of thioTEPA with HLMs and NADPH generating system (Fig. 12) and concur with our earlier report with S-mephenytoin N-demethylation (Rae et al., 2002), a probe of

JPET#49601

CYP2B6(Ko et al., 1998). Experiments were performed to assess if this inhibition of thioTEPA is mediated by metabolite-intermediate complex. ThioTEPA did not form any detectable MIC in pooled human liver microsomes or cDNA expressed CYP2B6 (data not shown). It is possible that the time-dependent effect of thioTEPA on CYP2B6 activity is due to its effect on CYP2B6 apoprotein. Of note, Hollenberg and his coworkers have identified numerous compounds that inactivate CYP2B6 by interfering with apoprotein [e.g. (Chun et al., 2000), (Kent et al., 1999)].

Discussion

We present here a detailed characterization of the *in vitro* human metabolism of efavirenz as summarized in Figure 13. We have demonstrated that: 1) efavirenz undergoes primary oxidative hydroxylation to 8-hydroxyefavirenz (major) and 7-hydroxyefavirenz (minor) and secondary metabolism to 8,14-dihydroxyefavirenz; 2) the major route of efavirenz metabolism is primarily catalyzed by CYP2B6; and 3) CYP2B6 exhibits atypical kinetics. These data should provide a scientific base upon which to build focused clinical studies that will help understand the pharmacokinetic and pharmacogenetic factors influencing efavirenz therapeutic efficacy, drug interactions and safety. Besides, efavirenz seems an attractive tool to study CYP2B6 activity *in vitro* and probably *in vivo*.

That 8-hydroxyefavirenz is the major metabolite of efavirenz *in vitro* is consistent with human studies in which this metabolite has been reported to be the principal metabolite of the drug (Mutlib et al., 1999). Glucuronide and sulfate conjugates of 7-hydroxyefavirenz have been identified in human urine (Mutlib et al., 1999), but the contribution of 7-hydroxylation to the overall clearance of efavirenz is likely to be small because the average Cl_{int} estimated from two HLMs for 7-hydroxylation reaction was >15-fold lower than that for 8-hydroxylation reaction. In addition to the two primary metabolites, we also identified 8,14-dihydroxyefavirenz as a secondary metabolite of efavirenz. According to Mutlib et al. (Mutlib et al., 1999), 8,14-dihydroxyefavirenz glucuronide has been detected in human plasma and urine. These authors proposed that efavirenz undergoes stepwise hydroxylation to form 8-hydroxyefavirenz and then to 8,14-dihydroxyefavirenz *in vivo* (Mutlib et al., 1999). We have shown that 8-hydroxyefavirenz was efficiently metabolized *in vitro* to 8,14-dihydroxyefavirenz. The time course for the formation of 8,14-dihydroxyefavirenz from efavirenz *in vitro* (present study) and *in vivo* (Mutlib et al., 1999) indicates a significant lag-time relative to that of 8-hydroxyefavirenz. Our findings provide direct evidence that 8,14-dihydroxyefavirenz is a secondary metabolite of efavirenz in that its formation proceeds stepwise from efavirenz, with 8-hydroxyefavirenz as intermediate. Based on our *in vitro* results (and assuming no further metabolism of 8,14-dihydroxyefavirenz and similar UV-absorbance intensity between the two

JPET#49601

metabolites), we estimate that ~17% of 8-hydroxyefavirenz formed from efavirenz is further oxidized to 8,14-dihydroxyefavirenz *in vitro*. The fraction is likely to be small *in vivo* where 8-hydroxyefavirenz might undergo rapid glucuronidation (Mutlib et al., 1999), although this claim needs experimental testing. Since the main source of 8,14-dihydroxyefavirenz *in vitro* seems 8-hydroxyefavirenz, the overall metabolism of efavirenz via the 8-hydroxylation route will be the summation of the formation of 8-hydroxyefavirenz (measured) and its subsequent 14-hydroxylation. When corrected for sequential metabolism, we would then predict substantially higher estimates of Cl_{int} for the overall 8-hydroxylation than those listed in Tables 1 and 3. Our *in vitro* data allow us to estimate that the contribution of total 8-hydroxylation pathway to the overall efavirenz oxidative metabolic clearance is >90%, with 7-hydroxylation playing a minor role.

The oxidation of efavirenz to 8-hydroxyefavirenz in HLMs is characterized by a sigmoidal substrate-velocity curve (Fig. 3) (Hill coefficient of 1.33-1.7), unlike the kinetic data obtained in recombinant human CYPs, which were characterized by a hyperbolic Michaelis-Menten equation (Fig. 7). Similar kinetic profile has been observed with another CYP2B6-mediated bupropion hydroxylation in HLMs (Faucette et al., 2000). Other recombinant CYP2B6-mediated reactions seem to depend on the substrate probe used: no autoactivation of efavirenz hydroxylation (present data) and bupropion hydroxylation (Faucette et al., 2000); or allosteric kinetics of 7-EFC O-deethylation (Ekins et al., 1997) and testosterone 16 β -hydroxylation (Ekins et al., 1998). The cause for the atypical kinetics for the formation of 8-hydroxyefavirenz from efavirenz in HLMs (but not in other CYPs) is unclear. Differences in membrane lipid composition, NADPH-P450 oxidoreductase and cytochrome b5 between the two systems could contribute to this. Moreover, although our *in vitro* data implicate CYP2B6 as the major enzyme catalyzing the sequential metabolism of efavirenz, the participation of CYPs other than CYP2B6 in HLMs cannot be excluded.

The formation of 8,14-dihydroxyefavirenz from efavirenz and 8-hydroxyefavirenz in HLMs and recombinant CYPs exhibited substrate inhibition. Similar substrate inhibition profiles have been observed previously with CYP3A-mediated triazolam (Schrag and Wienkers, 2001) and midazolam (Gorski et al., 1994)

regioselective hydroxylation, which are suggestive of multiple substrate-binding sites (or multiple regions within a single active site). To our knowledge, this is the first report of CYP2B6-mediated substrate inhibition. Although this observation may have no clinical relevance as it does not affect the initial 8-hydroxylation of efavirenz and because the expected *in vivo* steady-state concentrations of the substrate (efavirenz or 8-hydroxyefavirenz) after standard doses of efavirenz (Smith et al., 2001) are much lower than the substrate inhibition constants we obtained here, it may offer an insight in to the characteristics of the enzyme.

Although our inhibition data (Table 4) implicate multiple enzymes in the 7-hydroxylation of efavirenz and we observed, the specific enzymes responsible remain unclear, as we were unable to further confirm with experiments involving recombinant CYPs and correlation analysis. It may be that the sensitivity of the assay did not allow us to measure 7-hydroxyefaviraenz when recombinant CYP450s were used or this metabolite is catalyzed by CYPs other than those tested here or through other NADPH-dependent reactions. Because the contribution of 7-hydroxylation to the overall clearance of efavirenz is likely to be small, no further attempt was made identify the CYPs involved.

We provide strong evidence that efavirenz 8-hydroxylation and the subsequent oxidation to 8,14-dihydroxyefavirenz is predominantly catalyzed by CYP2B6. First, the formation rates of these metabolites from efavirenz were potently inhibited by thioTEPA (Table 4), a specific inhibitor of CYP2B6 (Rae et al., 2002). Second, CYP2B6 formed 8-hydroxyefavirenz and 8,14-dihydroxyefavirenz from efavirenz (Fig. 6) [and 8,14-dihydroxyefavirenz from 8-hydroxyefavirenz (Fig. 9)] with the highest specific activity. Third, the K_m value of 8-hydroxyefavirenz derived from HLMs (~20.2 μM) (Table 1) was similar to that observed in CYP2B6 (12.4 μM) (Table 3). Fourth, the formation rates of 8-hydroxyefavirenz (or 8,14-dihydroxyefavirenz) correlated significantly with the activity of CYP2B6 in a panel of HLMs (Table 2). We also noted that recombinant human CY1A2, CYP3A5 and CYP3A4 formed 8-hydroxyefavirenz from efavirenz, but the contributions of these isoforms to efavirenz metabolism appear minor: a) the Cl_{int} for 8-hydroxyefavirenz formation by CYP3A5, CYP1A2 and CYP3A4 were 5.8, 13.5- and 60-fold lower respectively (fold differences is larger when sequential metabolism is

JPET#49601

taken in to account) than that obtained in recombinant human CYP2B6 (Table 3); b) a CYP1A2 specific inhibitor (furafylline) and CYP3A specific inhibitors (ketoconazole and troleandomycin) did not inhibit the rates of formation of 8-hydroxyefavirenz or 8,14-dihydroxyefavirenz in HLMs and CYP2B6 (Table 4); and c) the disappearance of efavirenz (1 μ M) from microsomal incubates was catalyzed by CYP2B6 (but not by coincubation with recombinant human CYP3A4, CYP3A5 or CYP1A2). The significant correlation we observed between the activity CYP3A and efavirenz 8-hydroxylation in the panel of HLMs tested may not be due to the actual involvement of CYP3A in efavirenz metabolism. Because our inhibition and recombinant experiments do not support a significant role of CYP3A in efavirenz metabolism, the observed significant correlation between efavirenz metabolism and CYP3A is probably derived from the significant correlation between the activity of CYP3A and CYP2B6 (Spearman $r = 0.72$; $P=0.0234$) in the bank of human livers tested. Recently, Mouly et al (Mouly et al., 2002) reported that there was no correlation between efavirenz systemic exposure and hepatic CYP3A activity in healthy volunteers. It is also important to note that, clarithromycin, a known inhibitor of CYP3A in the gut-wall and the liver(Gorski et al., 1998), had negligible effect on the elimination of efavirenz in humans (Bristol-Myers Squibb Company, 2002) Besides, certain inhibitors and inducers of CYP3A had no or minimal effect on the elimination of efavirenz in humans (Product information, 2002).

Collectively, our *in vitro* data together with *in vivo* evidence from the literature strongly suggest that CYP2B6 is the principal catalyst of efavirenz metabolism (Fig. 13), which may have important implications for HIV/AIDs therapy. In human livers *in vitro*, wide interindividual variability in the expression of CYP2B6 is seen at the level of mRNA (Chang et al., 2003), protein (Code et al., 1997), (Faucette et al., 2000), (Lang et al., 2001), (Stresser and Kupfer, 1999) and catalytic activity (Faucette et al., 2000), (Ekins et al., 1998). This variability is probably due to effects of genetic polymorphisms of CYP2B6 (Ariyoshi et al., 2001), (Lang et al., 2001) or exposure to drugs that are inducers (Fauchette et al., 2001), (Sueyoshi and Negishi, 2001),(Gervot et al., 1999) or inhibitors (Rae et al., 2002),(Hesse et al., 2001) of CYP2B6. If our *in vitro* data can be extrapolated to *in vivo*

JPET#49601

conditions, we would expect that variability in efavirenz pharmacokinetics and drug interactions is primarily a reflection of the large interindividual differences in the activity of CYP2B6. It is now believed that ~8% of the drugs on the market are fully or partially metabolized by CYP2B6 (Treger JM and Stoll S, 2002) and it represents ~6% of the total liver CYP450 content (Stresser and Kupfer, 1999), in contrast to earlier estimates that it represented less than 1% (Shimada et al., 1994). Despite this and the identification of a growing list of clinically important drugs, environmental chemicals and endogenous substances as substrates of CYP2B6 *in vitro* (Wang and Halpert, 2002), (Ekins and Wrighton, 1999), it remains difficult to determine or predict its clinical consequences because of the unavailability of a specific and safe probe to measure the activity of the enzyme *in vivo*. Our data indicate that efavirenz 8-hydroxylation is a specific *in vitro* reaction marker of CYP2B6 and may have utility as a phenotyping tool to study the role of this enzyme in human drug metabolism.

References

- Ariyoshi N, Miyazaki M, Toide K, Sawamura Y, and Kamataki T (2001) A single nucleotide polymorphism of CYP2B6 found in Japanese enhances catalytic activity by autoactivation. *Biochem Biophys Res Commun.* **281**:1256-1260.
- Bradford MM (1976) A rapid and sensitive method for the quantitation of microgram quantities of protein utilizing the principle of protein-dye binding. *Anal Biochem* **72**:248-254.
- Product Information of Efavirenz (Sustiva), Bristol-Myers Squibb Company. April 2002.
- Chang TK, Bandiera SM, and Chen J (2003) Constitutive Androstane Receptor and Pregnane X Receptor Gene Expression in Human Liver: Interindividual Variability and Correlation with CYP2B6 mRNA Levels. *Drug Metab Dispos.* **31**:7-10.
- Chen H, Chen W, Gan LS, and Mutlib AE (2003) Metabolism of (S)-5,6-Difluoro-4-cyclopropylethynyl-4-trifluoromethyl-3,4-dihydro-2(1H)-quinazolinone, a Non-Nucleoside Reverse Transcriptase Inhibitor, in Human Liver Microsomes. Metabolic Activation and Enzyme Kinetics. *Drug Metab Dispos* **31**:122-132.
- Chun J, Kent UM, Moss RM, Sayre LM, and Hollenberg PF (2000) Mechanism-based inactivation of cytochromes P450 2B1 and P450 2B6 by 2-phenyl-2-(1-piperidinyl)propane. *Drug Metab Dispos* . **28**:905-911.
- Code EL, Crespi CL, Penman BW, Gonzalez FJ, Chang TK, and Waxman DJ (1997) Human cytochrome P4502B6: interindividual hepatic expression, substrate specificity, and role in procarcinogen activation. *Drug Metab Dispos* **25**:985-993
- Desta Z, Kerbusch T, Soukhova N, Richard E, Ko JW, and Flockhart DA (1998) Identification and characterization of human cytochrome P450 isoforms interacting with pimozone. *J Pharmacol Exp Ther.* **285** :428-437.

JPET#49601

Ekins S, Vandenbranden M, Ring BJ, Gillespie JS, Yang TJ, Gelboin HV, and Wrighton

SA (1998) Further characterization of the expression in liver and catalytic activity of CYP2B6. *J Pharmacol Exp Ther* **286**:1253-1259.

Ekins S, Vandenbranden M, Ring BJ, and Wrighton SA (1997) Examination of purported probes of human CYP2B6. *Pharmacogenetics* **7**:165-179.

Ekins S and Wrighton SA (1999) The role of CYP2B6 in human xenobiotic metabolism. *Drug Metab Rev* **31**:719-754.

Faucette SR, Hawke RL, Lecluyse EL, Shord SS, Yan B, Laethem RM, and Lindley CM (2000) Validation of bupropion hydroxylation as a selective marker of human cytochrome P450 2B6 catalytic activity. *Drug Metab Dispos* **28**:1222-1230.

Fauchette, S, Lindley, C, Hawke R, Shord S, Clarke M, and LeCluyse E (2001) Effects of cytochrome P450 (CYP) P450 3A inducers on CYP2B6 catalytic activity. *Clin Pharmacol Ther* **69**, 10..

Gervot L, Rochat B, Gautier JC, Bohnenstengel F, Kroemer H, de B, V, Martin H, Beaune P, and de W, I (1999) Human CYP2B6: expression, inducibility and catalytic activities. *Pharmacogenetics* **9**:295-306.

Gorski JC, Hall SD, Jones DR, Vandenbranden M, and Wrighton SA (1994) Regioselective biotransformation of midazolam by members of the human cytochrome P450 3A (CYP3A) subfamily. *Biochem Pharmacol* **47**:1643-1653.

Gorski JC, Jones DR, Haehner-Daniels BD, Hamman MA, O'Mara EM, Jr., and Hall SD (1998) The contribution of intestinal and hepatic CYP3A to the interaction between midazolam and clarithromycin. *Clin Pharmacol Ther* **64**:133-143.

Hesse LM, Von Moltke LL, Shader RI, and Greenblatt DJ (2001) Ritonavir, efavirenz, and nelfinavir inhibit CYP2B6 activity *in vitro*: potential drug interactions with bupropion. *Drug Metab Dispos* **29**:100-102

JPET#49601

Jones DR, Gorski JC, Hamman MA, Mayhew BS, Rider S, and Hall SD (1999) Diltiazem

inhibition of cytochrome P-450 3A activity is due to metabolite intermediate complex formation. *J Pharmacol Exp Ther* **290**:1116-1125.

Kennedy MJ, Armstrong DK, Huelskamp AM, Ohly K, Clarke BV, Colvin OM, Grochow LB, Chen TL, and

Davidson NE (1995) Phase I and pharmacologic study of the alkylating agent modulator novobiocin in combination with high-dose chemotherapy for the treatment of metastatic breast cancer. *J Clin Oncol* **13**:1136-1143.

Kent UM, Yanev S, and Hollenberg PF (1999) Mechanism-based inactivation of cytochromes P450 2B1 and P450 2B6 by n-propylxanthate. *Chem Res Toxicol* **12**:317-322.

Ko JW, Desta Z, and Flockhart DA (1998) Human N-demethylation of (S)-mephenytoin by cytochrome P450s 2C9 and 2B6. *Drug Metab Dispos* **26**:775-778.

Lang T, Klein K, Fischer J, Nussler AK, Neuhaus P, Hofmann U, Eichelbaum M, Schwab M, and Zanger UM

(2001) Extensive genetic polymorphism in the human CYP2B6 gene with impact on expression and function in human liver. *Pharmacogenetics* **11**:399-415.

Langmann P, Weissbrich B, Desch S, Vath T, Schirmer D, Zilly M, and Klinker H (2002) Efavirenz Plasma Levels for the Prediction of Treatment Failure in Heavily Pretreated HIV-1 Infected Patients. *Eur J Med Res* **7**:309-314.

Lopez-Cortes LF, Ruiz-Valderas R, Viciano P, Alarcon-Gonzalez A, Gomez-Mateos J, Leon-Jimenez E, Sarasanacenta M, Lopez-Pua Y, and Pachon J (2002) Pharmacokinetic Interactions Between Efavirenz and Rifampicin in HIV- Infected Patients with Tuberculosis. *Clin Pharmacokinet* **41**:681-690.

JPET#49601

Marzolini C, Telenti A, Decosterd LA, Greub G, Biollaz J, and Buclin T (2001) Efavirenz

plasma levels can predict treatment failure and central nervous system side effects in HIV-1-infected patients.

AIDS **15**:71-75.

McComsey G, Bhumbra N, Ma JF, Rathore M, and Alvarez A (2003) Impact of protease inhibitor substitution with efavirenz in HIV- infected children: results of the First Pediatric Switch Study. *Pediatrics* **111**:e275-e281.

Mouly S, Lown KS, Kornhauser D, Joseph JL, Fiske WD, Benedek IH, and Watkins PB (2002) Hepatic but not intestinal CYP3A4 displays dose-dependent induction by efavirenz in humans. *Clin Pharmacol Ther* **72**:1-9.

Mutlib AE, Chen H, Nemeth GA, Markwalder JA, Seitz SP, Gan LS, and Christ DD (1999b) Identification and characterization of efavirenz metabolites by liquid chromatography/mass spectrometry and high field NMR: species differences in the metabolism of efavirenz. *Drug Metab Dispos* **27**:1319-1333.

Rae JM, Soukhova NV, Flockhart DA, and Desta Z (2002) Triethylenethiophosphoramidate is a specific inhibitor of cytochrome P450 2B6: implications for cyclophosphamide metabolism. *Drug Metab Dispos* **30**:525-530.

Schrag ML and Wienkers LC (2001) Triazolam substrate inhibition: evidence of competition for heme-bound reactive oxygen within the CYP3A4 active site. *Drug Metab Dispos* **29**:70-75.

Shimada T, Yamazaki H, Mimura M, Inui Y, and Guengerich FP (1994) Interindividual variations in human liver cytochrome P-450 enzymes involved in the oxidation of drugs, carcinogens and toxic chemicals: studies with liver microsomes of 30 Japanese and 30 Caucasians. *J Pharmacol Exp Ther* **270**:414-423.

Smith PF, DiCenzo R, and Morse GD (2001) Clinical pharmacokinetics of non-nucleoside reverse transcriptase inhibitors. *Clin Pharmacokinet* **40**:893-905.

Staszewski S, Morales-Ramirez J, Tashima KT, Rachlis A, Skiest D, Stanford J, Stryker R, Johnson P, Labriola DF, Farina D, Manion DJ, and Ruiz NM (1999) Efavirenz plus zidovudine and lamivudine, efavirenz plus

JPET#49601

indinavir, and indinavir plus zidovudine and lamivudine in the treatment of HIV-1 infection in adults. Study 006 Team. *N Engl J Med* **341**:1865-1873.

Stresser DM and Kupfer D (1999) Monospecific antipeptide antibody to cytochrome P-450 2B6. *Drug Metab Dispos* **27**:517-525.

Sueyoshi T and Negishi M (2001) Phenobarbital response elements of cytochrome P450 genes and nuclear receptors. *Annu Rev Pharmacol Toxicol* **41**:123-143.

Taylor S, Reynolds H, Sabin CA, Drake SM, White DJ, Back DJ, and Pillay D (2001) Penetration of efavirenz into the male genital tract: drug concentrations and antiviral activity in semen and blood of HIV-1- infected men. *AIDS* **15**:2051-2053.

Treger JM and Stoll S (2002) Cytochrome P450: their impact on drug treatment. *Hospital Pharmacist* 167-173.

Von Moltke LL, Greenblatt DJ, Granda BW, Giancarlo GM, Duan SX, Daily JP, Harmatz JS, and Shader RI (2001) Inhibition of human cytochrome P450 isoforms by nonnucleoside reverse transcriptase inhibitors. *J Clin Pharmacol* **41**:85-91.

Wang Q and Halpert JR (2002) Combined three-dimensional quantitative structure-activity relationship analysis of cytochrome P450 2B6 substrates and protein homology modeling . *Drug Metab Dispos*. **30**:86-95.

Wynn HE, Brundage RC, and Fletcher CV (2002) Clinical implications of CNS penetration of antiretroviral drugs. *CNS Drugs* **16**:595-609.

JPET#49601

Footnotes

The study was funded by the National Institute of General Medical Sciences grants RO1-GM56898-01 and T32 GM 56898, Bethesda, MD

Reprint request to:

Zeruesenay Desta, Ph.D.

Assistant Professor of Medicine and Pharmacology and Toxicology

Indiana University School of Medicine, Department of Medicine

Division of Clinical Pharmacology

1001 West 10th Street, WD Myers Bldg., W7123

Indianapolis, IN 46202

Telephone: (317) 630 8860 Fax: (317) 630 8185

E-mail: zdesta@iupui.edu

Legends for figures

Figure 1. HPLC traces of efavirenz and its metabolites from *in vitro* incubation with HLMs. Efavirenz (10 μ M) was incubated with HLMs (0.5 mg/ml protein) and a NADPH-generating system for 30 min at 37°C. The appearances of metabolite peaks were monitored by HPLC with UV-detection (see Methods).

Figure 2. Time course for the formation of efavirenz metabolites in HLMs. Efavirenz (5 μ M) was incubated in HLMs (0.5mg/ml) and a NADPH generating system (final volume, 250 μ M) at 37°C. Reaction was terminated at time = 0 and after 5, 10, 15, 20, 30, 45 and 60 min of incubation.

Figure 3. Kinetics for the formation rate of 8-hydroxyefavirenz from efavirenz in two HLMs (HL9 and HL14/09/99). An increasing concentration of efavirenz (0-200 μ M) was incubated with HLMs (0.5 mg/ml) and a NADPH-generating system for 30 min at 37°C. **Left panel:** rate of formation of MI (8-hydroxyefavirenz) (pmol/min/mg protein) vs. efavirenz concentration curves where the kinetic data were fit to a Hill equation (see Data Analysis); and **right panel**, the corresponding Eadie-Hofstee plots (rate vs. rate/efavirenz concentrations). Each point represents average of duplicate incubations.

Figure 4. Kinetics for the formation rate of 8,4-dihydroxyefavirenz from 8-hydroxyefavirenz in HLMs (HL112). An increasing concentration of 8-hydroxyefavirenz (0-200 μ M) was incubated with HLMs (0.5 mg/ml) and a NADPH-generating system for 30 min at 37°C. The kinetic data [rate of formation of 8,14-dihydroxyefavirenz (pmol/min/mg protein) vs. efavirenz concentrations] were fit to a substrate inhibition equation (see Data Analysis). The corresponding Eadie-Hofstee plot (velocity vs. velocity/8-hydroxyefavirenz concentrations) is shown in the insert. Each point represents average of duplicate incubations.

JPET#49601

Figure 5. The rate of efavirenz metabolism in a panel of 11 characterized HLMs. Efavirenz (10 μ M) was incubated with microsomes from different human livers (0.5 mg/ml) and a NADPH generating system for 30 min at 37°C. Data are average of duplicate incubations. The correlation between the rates of formation MI (8-hydroxyefavirenz), MII (7-hydroxyefavirenz) and MIII (8,14-dihydroxyefavirenz) from efavirenz and the activity of each CYP isoform is illustrated in Table 2.

Figure 6. Metabolism of efavirenz to 8-hydroxyefavirenz (MI) and 8,14-dihydroxyefavirenz (MIII) by a panel of recombinant human CYPs. Efavirenz (10 μ M) was incubated with a panel of recombinant human CYP450 isoforms (52 pmol/ml) and a NADPH-generating system at 37°C for 30 min. Data are presented as mean \pm SD (pmol product/min/pmol of P450) of 4 measurements at two different days. 7-Hydroxyefavirenz was formed by none of the isoforms tested.

Figure 7. The formation of 8-hydroxyefavirenz (MI) and 8,14-dihydroxyefavirenz (MIII) from efavirenz in recombinant human CYP2B6. An increasing concentration of efavirenz (0-200 μ M) was incubated with recombinant CYP2B6 (52 pmol/ml) and a NADPH-generating system (incubation condition as in Fig. 6). **Left panel**, velocity (pmol/min/pmol P450) vs. substrate curves, where the data of 8-hydroxyefavirenz and 8,14-dihydroxyefavirenz were fit to a Michaelis-Menten and substrate inhibition equations respectively (see Data Analysis); and **right panel**, the corresponding Eadie-Hofstee plots (velocity vs. velocity/substrate concentration). Each point represents average of duplicate incubations.

Figure 8. Kinetics for the formation rate of 8-hydroxyefavirenz (MI) from efavirenz in recombinant human CYP2B6, CYP1A2, CYP3A5 and CYP3A. An increasing concentration of efavirenz (0-200 μ M) was incubated with recombinant human CYP2B6, CYP1A2 and CYP3A5 (52 pmol/ml) and a NADPH-generating system at

JPET#49601

37°C for 30 min. The velocity (pmol/min/pmol P450) vs. efavirenz concentration was fit to

a Michaelis-Menten equation (see Data Analysis). Each point represents average of duplicate incubations.

Figure 9. Metabolism of 8-hydroxyefavirenz to 8,14-dihydroxyefavirenz by a panel of cDNA-expressed human CYP450 isoforms. 8-Hydroxyefavirenz (2.5 μ M) was incubated with a panel of recombinant human CYP450 isoforms (52 pmol/ml) and a NADPH-generating system at 37°C for 30 min. Data are presented as mean (pmol product/min/pmol of P450) of duplicate measurements.

Figure 10. Kinetics for the formation 8,4-dihydroxyefavirenz from 8-hydroxyefavirenz in recombinant CYP2B6. An increasing concentration of 8-hydroxyefavirenz (0-200 μ M) was incubated with CYP2B6 (52 pmol/ml) and a NADPH-generating system for 30 min at 37°C. The kinetic data [rate of formation of 8,14-dihydroxyefavirenz (pmol/min/pmol P450) vs. 8-hydroxyefavirenz concentrations] were fit to a substrate inhibition equation (see Data Analysis). The corresponding Eadie-Hofstee plot (velocity vs. velocity/8-hydroxyefavirenz concentrations) is shown in the insert. Each point represents average of duplicate incubations.

Figure 11. Dixon plots for the inhibition of efavirenz metabolism to MI (8-hydroxyefavirenz) by thioTEPA in HLMS. Efavirenz (5-25 μ M) was incubated without or with thioTEPA (2.5-10 μ M) in HLMS and a NADPH-generating system at 37°C for 30 min. Each point represents mean of duplicate measurements.

Figure 12. Effect of preincubation of thioTEPA on the rate of formation of MI (8-hydroxyefavirenz), MII (7-hydroxyefavirenz) and MIII (8,14-dihydroxyefavirenz) from efavirenz in HLMS. ThioTEPA (5 μ M) was preincubated (0-30 min) in HLMS (0.5 mg/ml) and an NADPH-generating system before the reactions were initiated with the addition of efavirenz (10 μ M) and further incubated for 30 min at 37°C. The effect of

JPET#49601

preincubation (%) was calculated by dividing the velocity at each specific preincubation time by the velocity at a preincubation time of zero. Data represent mean \pm SD (n=3 independent experiments with duplicates).

Figure 13. Proposed human metabolism of efavirenz.

Table 1: Kinetic parameters for the formation of 8-hydroxyefavirenz (MI) and 7-hydroxyefavirenz (MII) from efavirenz in two HLMs.

Kinetic parameters	HL9		HL9/14/99	
	MI	MII	MI	MII
V _{max}	122.4 (3.9)	5.5 (0.2)	157.4 (4.7)	32.5 (3.5)
K _m	17.4 (1.5)	13.1 (1.8)	22.9 (1.2)	66.6 (13.9)
Hill coefficient	1.33 (0.1)		1.7 (0.1)	
V _{max} /K _m	7.0	0.4	6.9	0.5

V_{max}, pmol/min/mg protein; K_m, μM; and V_{max}/K_m, μL/min/mg protein). Kinetic parameters for the formation of 8-hydroxyefavirenz were estimated by fitting the velocity vs. substrate concentrations to Hill equation and for the formation of 7-hydroxyefavirenz using a single site Michaelis-Menten equation. Apparent kinetic parameters (standard errors of parameter estimates) are presented.

JPET#49601

Table 2: Correlation of formation rates of 8-hydroxyefavirenz (MI), 7-hydroxyefavirenz (MII), 8,14-dihydroxyefavirenz (MIII) from efavirenz (10 μ M) with the activities of different CYP isoforms, total P450 contents in 11 HLMs. Data were analyzed using the nonparametric correlation test (Spearman *r*). The activity of each isoform determined using the respective specific substrate probe reaction was as supplied by the supplier (see Methods Section). *P* = 0.05 is considered statistically significant.

CYPs	Metabolites of efavirenz							
	MI		MII		MIII		MI+MIII	
	<i>r</i>	<i>p</i>	<i>r</i>	<i>p</i>	<i>r</i>	<i>p</i>	<i>r</i>	<i>p</i>
Total P450	0.65	0.049	-0.1	0.79	0.66	0.044	0.65	0.049
OR	0.43	0.22	0.42	0.23	0.47	0.18	0.43	0.22
Cyt. B5	-0.44	0.2	0.47	0.18	-0.45	0.19	-0.44	0.2
1A2	-0.16	0.66	0.02	0.97	-0.25	0.49	-0.17	0.66
2A6	0.20	0.58	0.45	0.19	0.42	0.23	0.20	0.58
2B6	0.77	0.013	-0.31	0.39	0.72	0.02	0.77	0.013
2C8	0.66	0.044	0.26	0.47	0.61	0.067	0.66	0.044
2C9	0.15	0.68	0.20	0.58	0.26	0.47	0.15	0.68
2C19	0.16	0.66	0.08	0.84	0.07	0.87	0.16	0.66
2D6	-0.16	0.66	-0.01	1.0	-0.07	0.87	-0.16	0.66
2E1	0.49	0.15	0.04	0.91	0.58	0.088	0.49	0.15
3A	0.85	0.003	0.09	0.8	0.95	0.0001	0.85	0.003
4A	0.05	0.89	0.6	0.07	-0.06	1.0	0.05	0.89

Table 3: Kinetic parameters for the formation of 8-hydroxyefavirenz from efavirenz in recombinant human CYPs.

Kinetic parameters	CYP2B6*	CYP2B6+b5**	CYP1A2**	CYP3A5**	CYP3A4**
V_{\max}	5.20±0.76	3.50 (0.07)	0.60 (0.04)	0.60 (0.03)	0.16 (0.01)
K_m	12.40±1.80	6.40 (0.5)	8.30 (2.40)	19.10 (3.14)	23.50 (3.10)
V_{\max}/K_m	0.42±0.06	0.55	0.07	0.03	0.007

Kinetic data are presented as *mean ±SD (n=3 independent experiments performed in duplicate) or **parameter estimated with standard error of parameter estimates obtained from WinNonlin in bracket. V_{\max} , pmol/min/pmol P450; K_m , μM; and V_{\max}/K_m , μL/min/pmol P450. Kinetic parameters were estimated by fitting the velocity vs. substrate concentrations to single site Michaelis-Menten equation. .

Table 4. Inhibition of efavirenz metabolism by P450 isoform-specific

inhibitors in HLMs and recombinant human CYP2B6. Efavirenz (10 μ M) was reconstituted in phosphate buffer (pH, 7.4) and incubated at 37°C for 30 min with microsomes from human liver or recombinant CYP2B6 and NADPH-generating system in the presence or absence of specific inhibitors. In HLMs, data represent % of control (without inhibitor) activity in HLMs (mean \pm S.D., $n = 2$ independent experiments measured in duplicate), while in recombinant CYP2B6 it is the average % of control activity of duplicate measurements.

	MI		MII*	MIII	
	HLMs	CYP2B6	HLMs	HLMs	CYP2B6
Control (no inhibitor)	100	100	100	100	100
Furafylline (20 μ M)	97 \pm 9.8	108.5	103.8 \pm 3.7	92.0 \pm 7.9	88.4
ThioTEPA (50μM)	35\pm1.3	40\pm3.5	143.3\pm5	25\pm1.6	22
Sulfaphenazole (20 μ M)	80.6 \pm 3.6	107.7	56 \pm 5.1	92.2 \pm 4.8	89.3
Omeprazole (10 μ M)	80.6 \pm 5.7	107.1	58.7 \pm 1.4	83.5 \pm 1.6	100.3
Quinidine (1 μ M)	83.9 \pm 1.9	97.5	79.2 \pm 18.6	95.8 \pm 0.5	95.3
DEDTC (50 μ M)	94.4 \pm 13.9	115.3	64.9 \pm 16	89.4 \pm 11.9	72.4
Ketoconazole (1 μ M)	82.8 \pm 4.2	104.7	100.5 \pm 16.4	86.3 \pm 4.4	80.2
Troleandomycin (50 μ M)	101.8 \pm 10.9	101.0	48.6 \pm 6.9	80.7 \pm 6.2	109.9

*MII was formed in HLMs, but not by CYP2B6; Inhibition data in HLMs were presented as mean \pm SD ($n =$ at least 3 independent experiments in duplicate), while the data from CYP2B6 are given as average of duplicate measurements.

Fig. 1

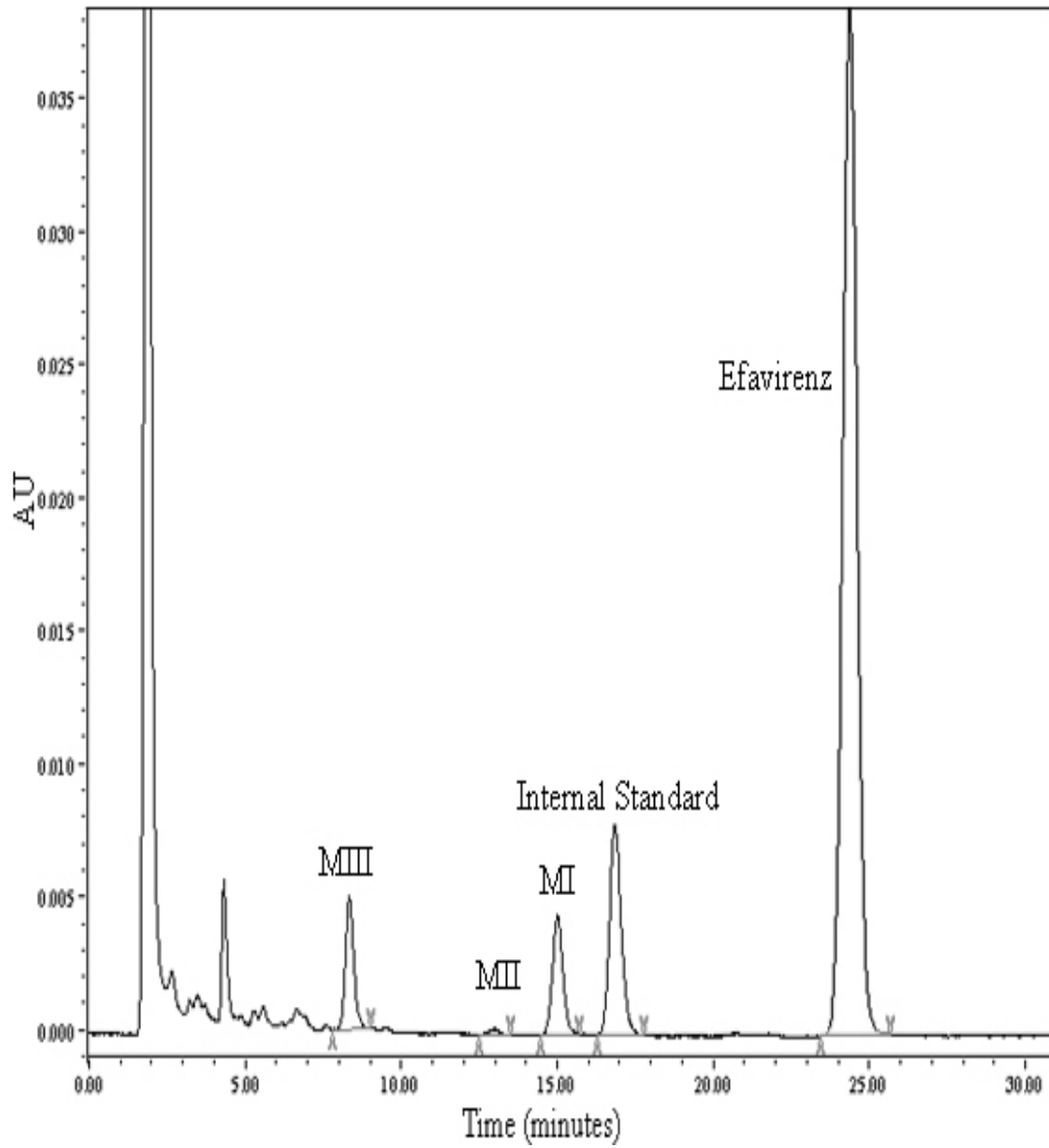


Fig. 2

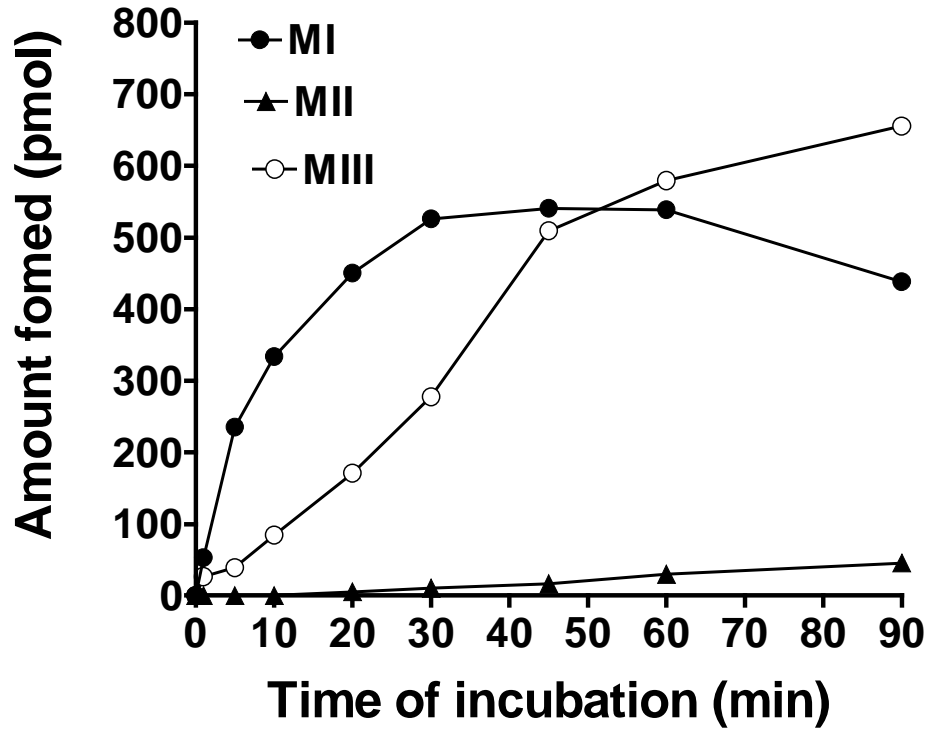


Fig. 3

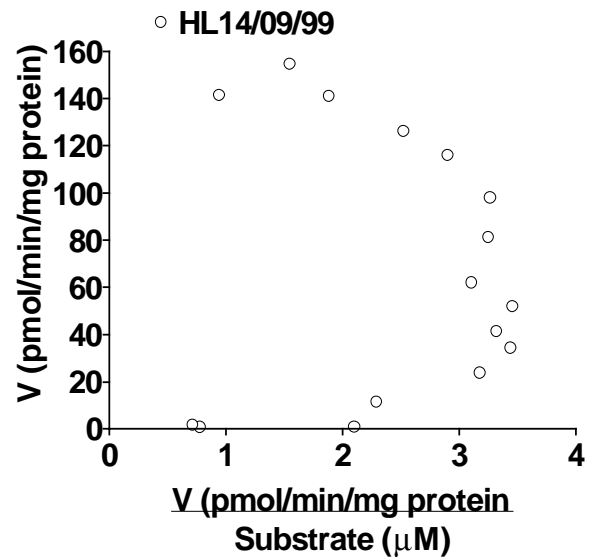
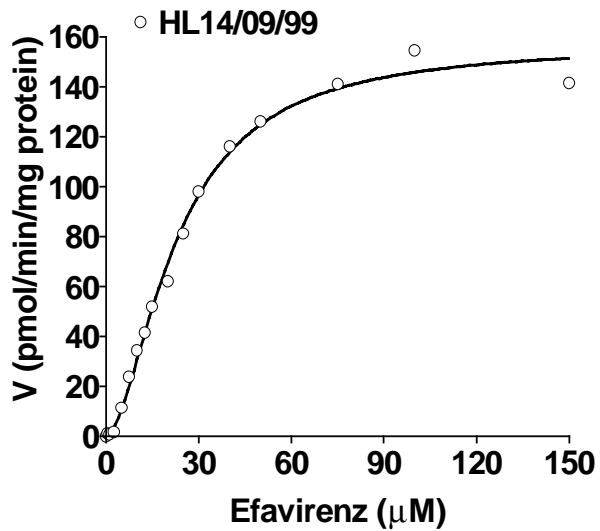
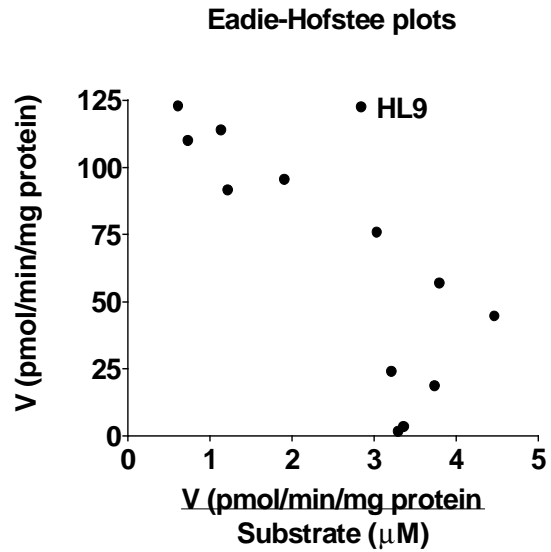
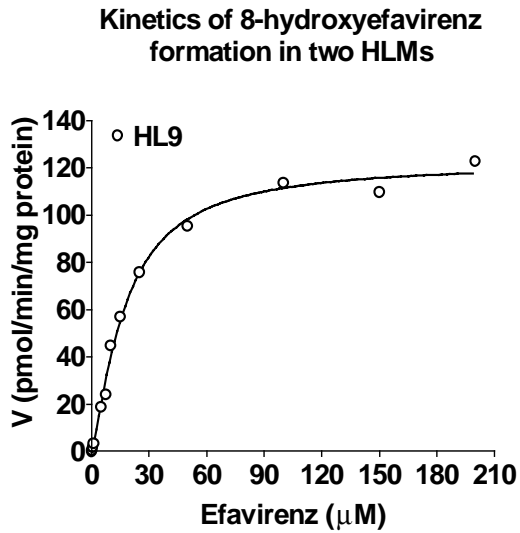
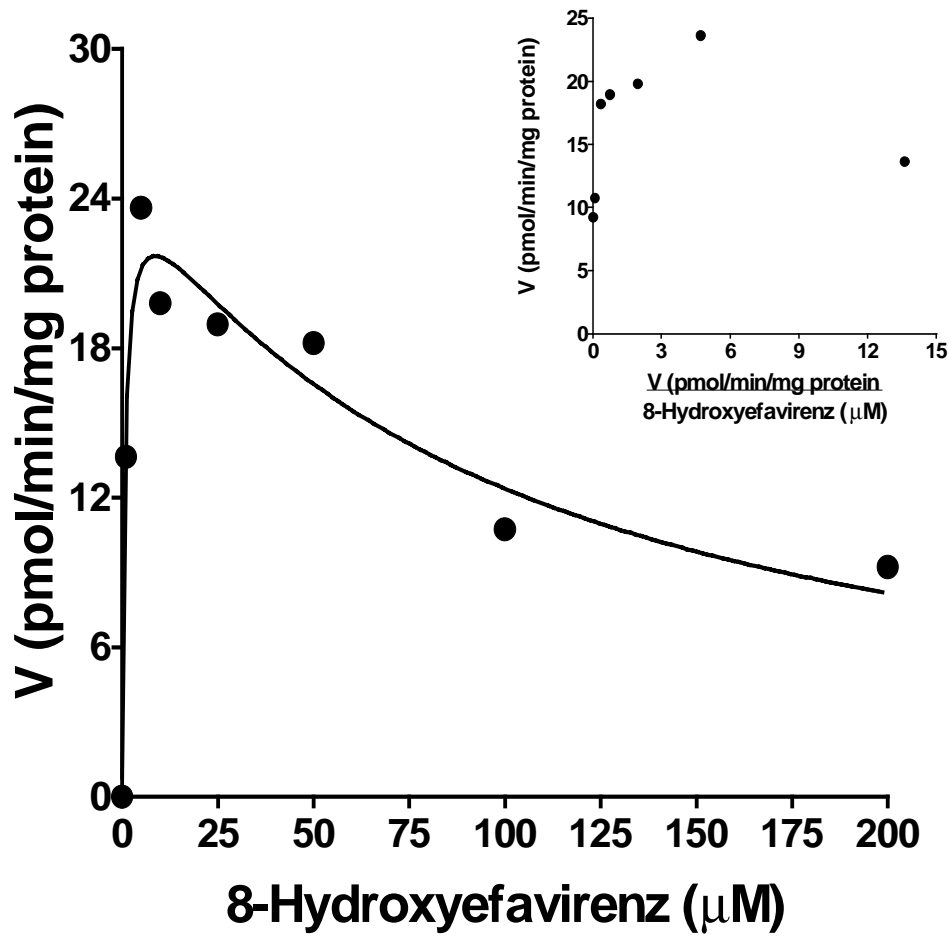


Fig. 4



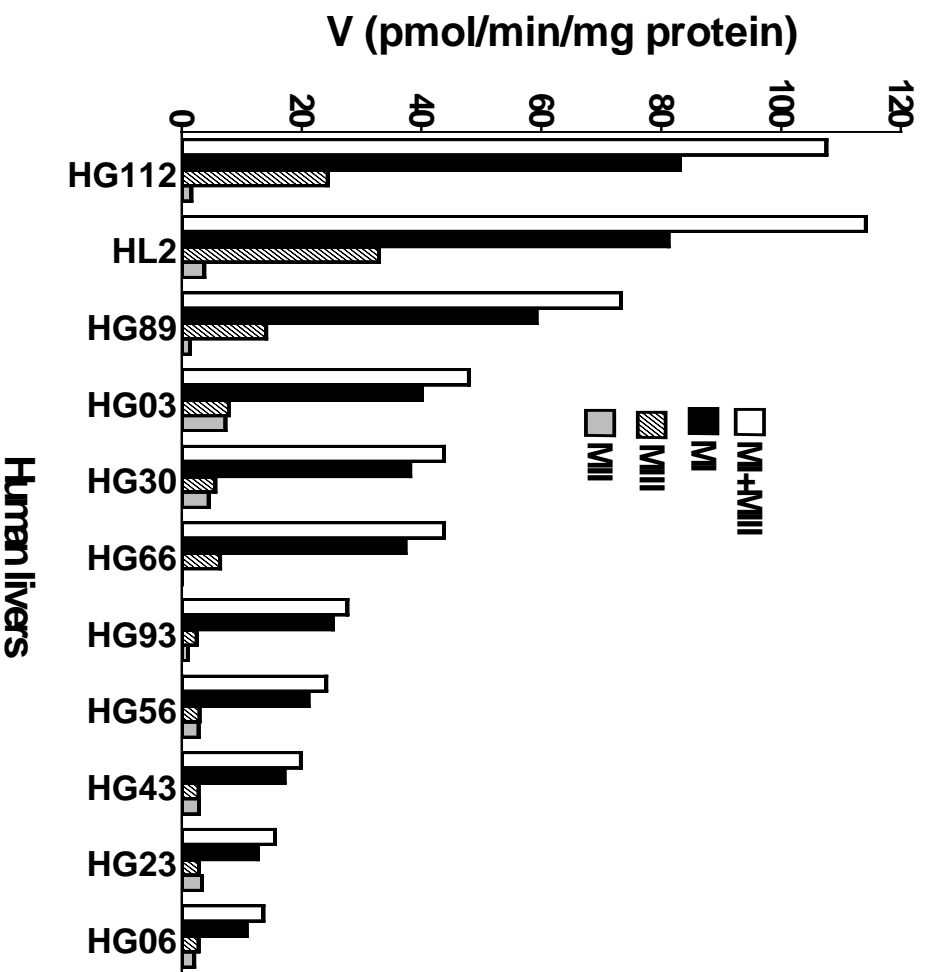


Fig. 5

Fig. 6

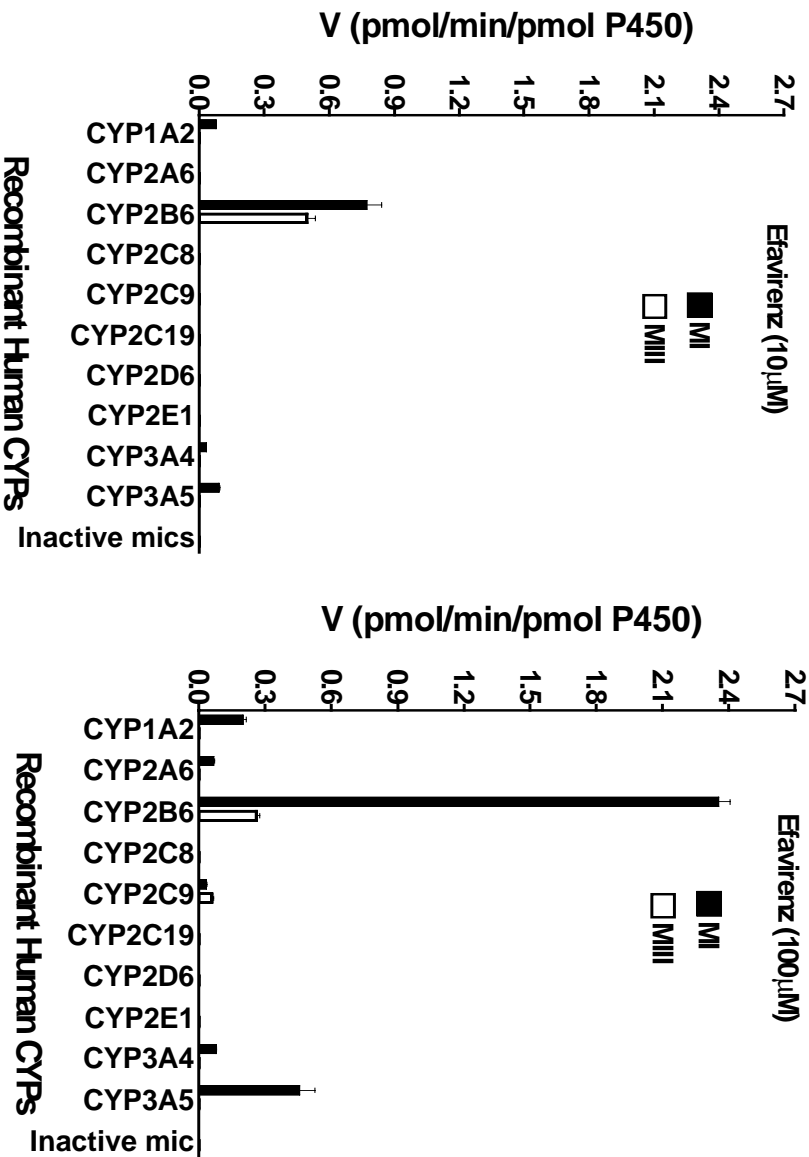


Fig. 7

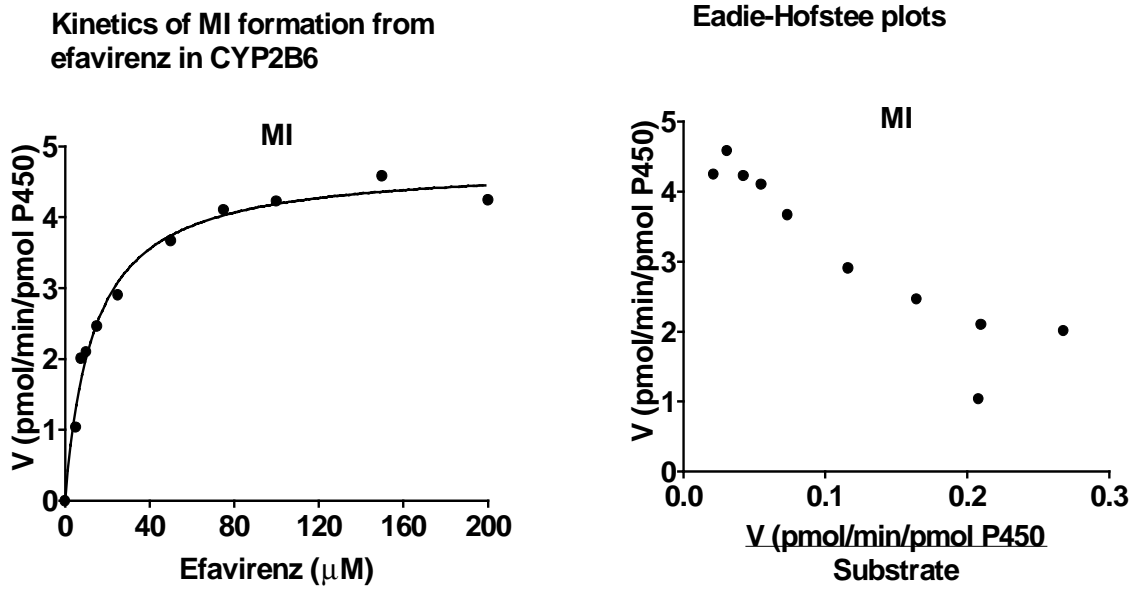


Fig. 8

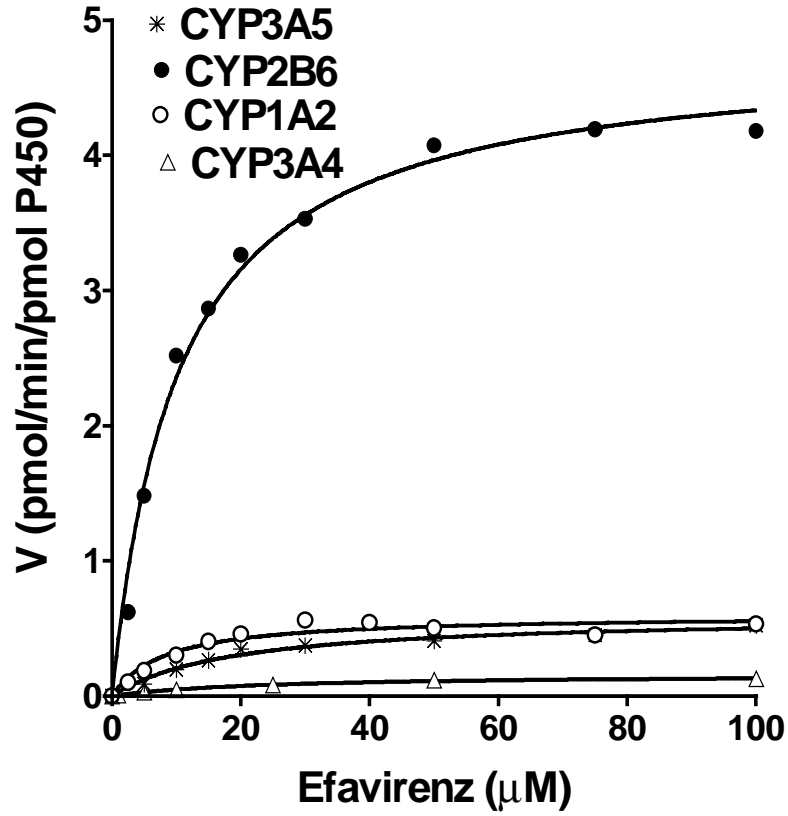


Fig. 9

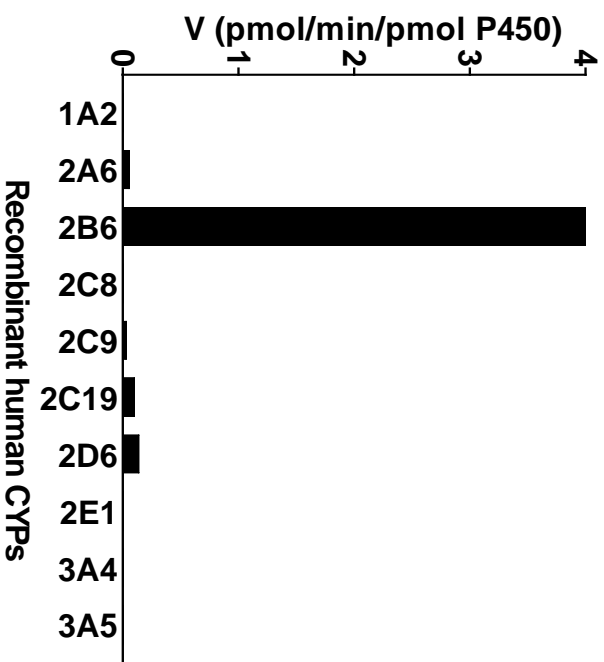


Fig. 10

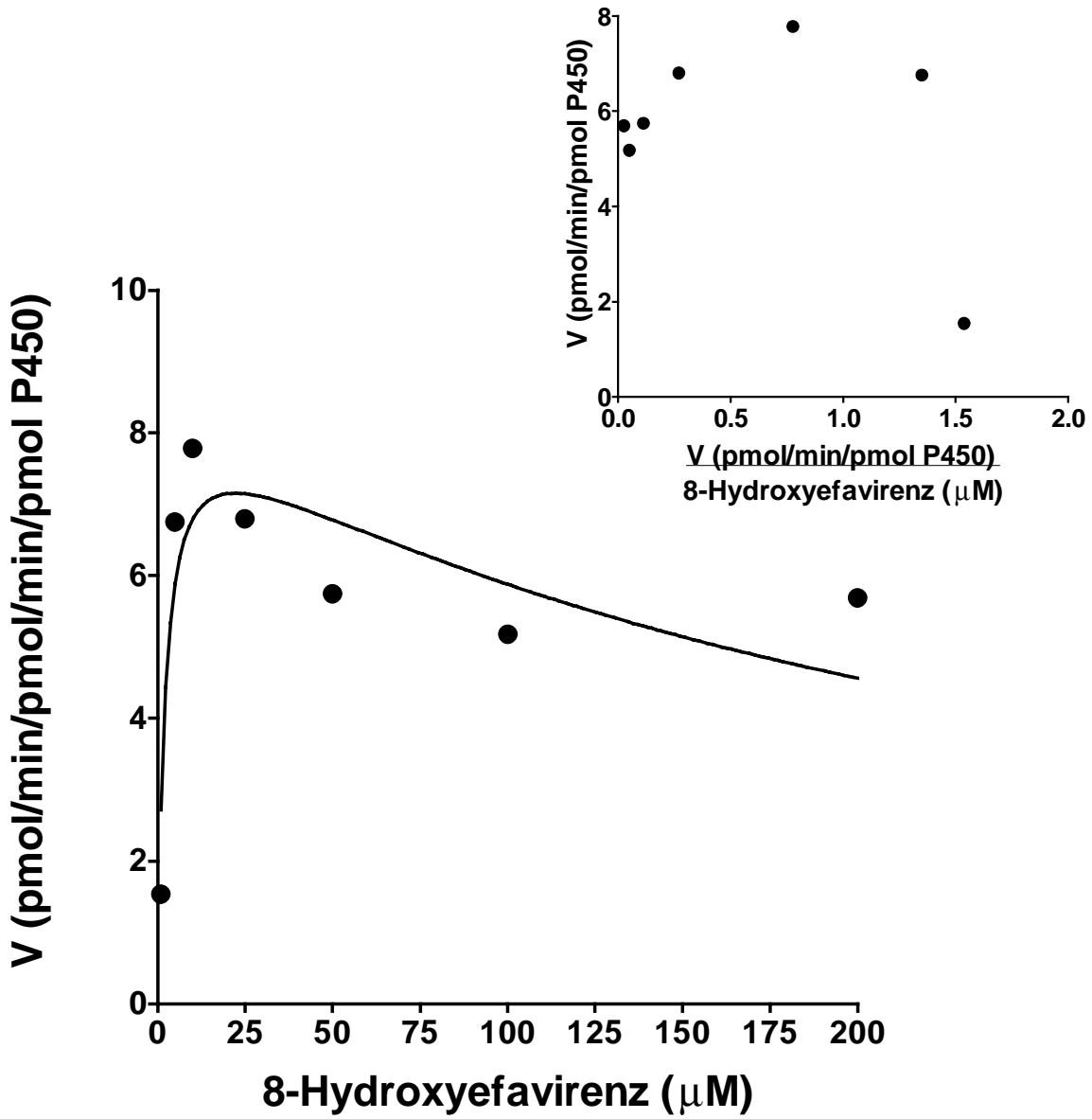


Fig. 11

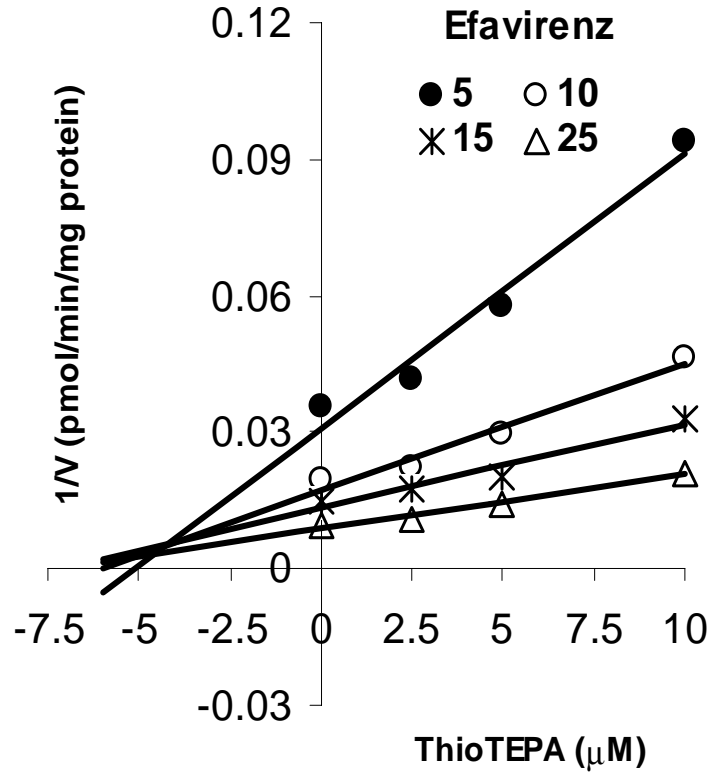


Fig. 12

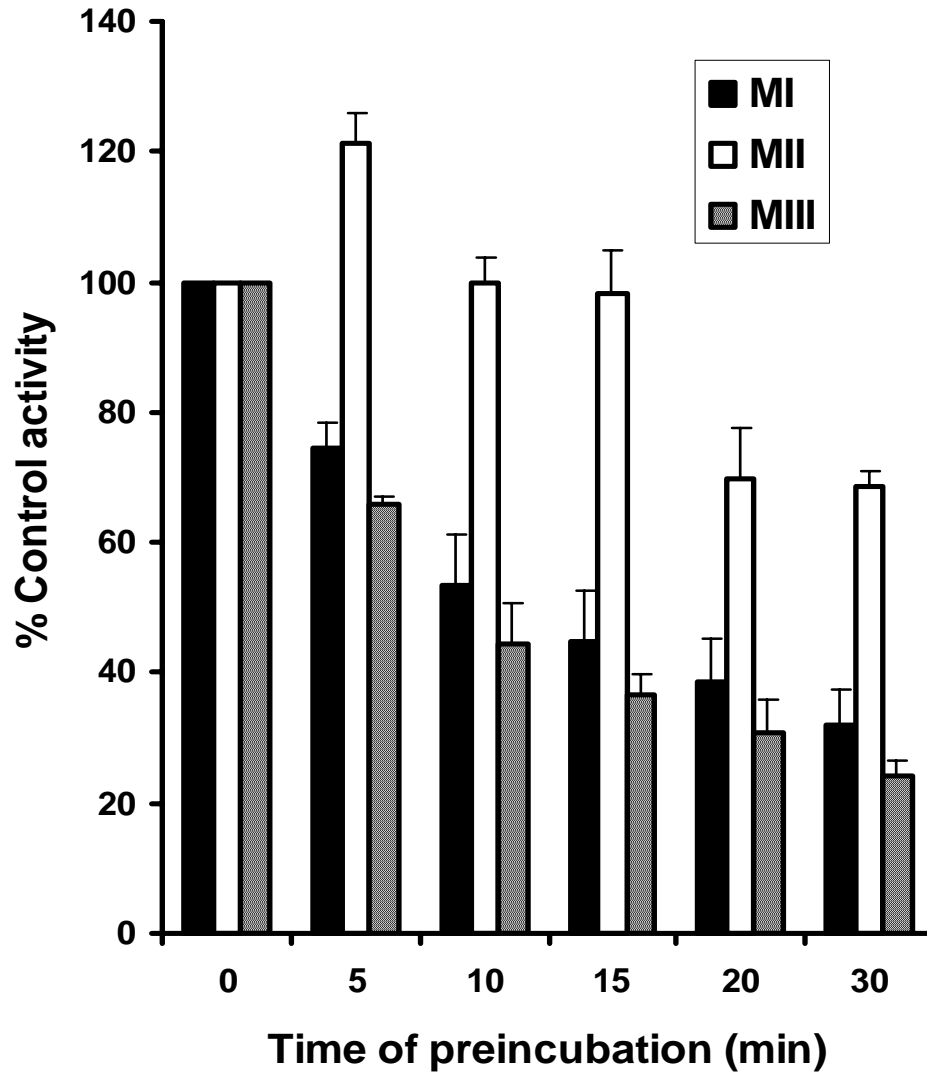


Fig. 13

